Innate Immune-gene expression during experimental Amyloodiniosis in European seabass (*Dicentrarchus labrax*)

Omkar Byadgi[1,*], Michela Massimo[1], Ron P Dirks[2], Alberto Pallavicini[3,4], James E Bron[5], Jacquie H Ireland[5], Donatella Volpatti[1], Marco Galeotti[1], Paola Beraldo[1]

[1]*Section of Animal and Veterinary Sciences, Department of Agricultural, Food, Environmental and Animal Sciences (DI4A), University of Udine, 33100 Udine, Italy.*

[2] *Future Genomics Technologies B.V., Leiden, The Netherlands.*

[3]*Laboratory of Genetics, Department of Life Sciences, University of Trieste, Via Licio Giorgeri 5, 34126 Trieste, Italy.*

[4]*National Institute of Oceanography and Applied Geophysics, via Piccard 54, 34151, Trieste, Italy.*

[5]*Institute of Aquaculture, University of Stirling, Stirling, Scotland, UK.*

∗ *Corresponding author. Omkar Byadgi, Section of Animal and Veterinary Sciences, Department of Agricultural, Food, Environmental and Animal Sciences (DI4A), University of Udine, 33100 Udine, Italy. Tel: +393917580339, E-mail: omkar.byadgi@uniud.it*

Abstract

The ectoparasite protozoan *Amyloodinium ocellatum* (AO) is the causative agent of amyloodiniosis in European seabass (ESB, *Dicentrarchus labrax*). There is a lack of information about basic molecular immune response mechanisms of ESB during AO infestation. Therefore, to compare gene expression between experimental AO-infested ESB tissues and uninfested ESB tissues (gills and head kidney) RNA-seq was adopted. The RNA-seq revealed multiple differentially expressed genes (DEG), namely 679 upregulated genes and 360 downregulated genes in the gills, and 206 upregulated genes and 170 downregulated genes in head kidney. In gills, genes related to the immune system (perforin, CC1) and protein binding were upregulated. Several genes involved in IFN related pathways were upregulated in the head kidney. Subsequently, to validate the DEG from amyloodiniosis, 26 ESB (mean weight 14g) per tank in triplicate were bath challenged for 2h with AO (3.5×10^6/tank; 70 dinospores/ml) under controlled conditions (26-28°C and 34‰ salinity). As a control group (non-infested), 26 ESB per tank in triplicate were also used. Changes in the expression of innate immune genes in gills and head kidney at 2, 3, 5, 7 and 23 dpi were analysed using real-time PCR. The results indicated that the expression of cytokines (CC1, IL-8) and antimicrobial peptide (Hep) were strongly stimulated and reached a peak at 5 dpi in the early infestation stage, followed by a gradual reduction in the recovery stage (23 dpi). Noticeably, the immunoglobulin (IgM) expression was higher at 23 dpi compared to 7 dpi. Furthermore, *in-situ* hybridization showed positive signals of CC1 mRNA in AO infested gills compared to the control group. Altogether, chemokines were involved in the immune process under AO infestation and this evidence allows a better understanding of the immune response in European seabass during amyloodiniosis.

***Keywords*:** *Amyloodinium ocellatum*, Dinoflagellates, Ectoparasite, Innate immunity, Illumina RNA-seq

1. Introduction

The ectoparasite dinoflagellate *Amyloodinium ocellatum* (AO) is one of the most problematic parasites causing disease among brackish and marine water fish, known as marine velvet disease (Brown EM., 1934). AO causes a parasitic branchitis associated with high mortality and significant economic losses in farming conditions worldwide (Cruz-Lacierda et al., 2004; Fioravanti et al., 2006; Benetti et al., 2008; Saraiva et al., 2011; Soares et al., 2011; Dequito et al., 2015; Gomez et al., 2018; Byadgi et al., 2019). This parasite mainly infests the gills, skin, and entire oropharyngeal cavity of almost all species of brackish and marine water fish, including European seabass (*Dicentrarchus labrax*) (Benetti et al., 2008; Alvarez-Pellitero, P et al., 1993; Byadgi et al., 2019).

Fish surviving the infestation may develop protective immunity, which suggests that the immunoprophylactic control of this disease through vaccination could be feasible (Smith et al., 1994; Cobb et al., 1998; Cecchini et al., 2001). However, the information regarding host responses to *A. ocellatum* infestation is limited (Byadgi et al., 2019).

Transcriptomics has been used extensively to explore the host response towards fish parasite infestations (Sudhagar et al., 2018). Results from the large yellow croaker (*Larimichthys polyactis*) after *Cryptocaryon irritans* infestation indicated enrichment of the Toll-like receptor pathway (TLR), chemokine signalling, complement system and coagulation cascades (Wang et al., 2016). Low, non-lethal infestation by *C. irritans* enhanced a significant local immune response in large yellow croaker (*Larimichthys crocea*) and induced immunosuppression (Yin et al., 2016). Similarly, in skin of orange spotted grouper (*Epinephelus coioides*) affected by *C. irritans,* a local immune response with intense leukocytes recruitment was observed (Hu et al., 2017). Interestingly, three-spined stickleback (*Gasterosteus aculeatus*) infested by three different genotypes of the trematode parasite, *Diplostomum pseudospathaceum,* revealed differential mechanisms by which the host immune system reacts to the immunological threat (Haase et al., 2016 & 2017). Moreover, in large yellow croaker upon infestation with the intestinal myxozoan parasite *Enteromyxum scophthalmi* an inadequate adaptive immune activation was observed (Robledo et al., 2014). However, during early phase of infestation in turbot (*Scophthalmus maximus)* by *E. scophthalmi* an IFN-mediated immune response was recorded (Ronza et al., 2016). During mild natural infestation of *Sparicotyle chrysophrii* in Gilthead sea bream (*Sparus aurata*) a strong enrichment of differentially expressed genes in gills, related to apoptosis, inflammation and cell proliferation was observed, whereas inhibition of DEG related to apoptosis, autophagy, platelet activation, signalling and aggregation in the spleen was observed (Piazzon et al., 2019). *Ichthyophthirius multifiliis* infestation in rainbow trout (*Oncorhynchus mykiss*) gills triggered an innate immune response by enhancing the Chemokine signalling pathway, platelet activation, Toll-like receptor signalling (TLR) pathway, NOD-like receptor signalling pathway, and Leukocyte transendothelial migration (Syahputra et al., 2019). RNA-Seq-based transcriptome analyses were also employed to study the parasites themselves such as *C. irritans* (Yin et al., 2016; Mo et al., 2016) and salmon louse *Caligus rogercresseyi* (Allardo-Escárate et al., 2014), in order to understand the host-parasite antigens interactions and to identify potential vaccine candidates.

Previous studies have indicated that Interleukin-1 (IL-1) and Tumor Necrosis Factor α (*Tnf-α*) were activated in infested ESB reared in an aquaponics system (Nozzi et al., 2016). Experimental infestation of AO in yellowtail (*Seriola lalandi*) enhanced the TLR22 expression and involved in response to AO infestation (Reyes-Becerril, M et al., 2015). Moreover, natural outbreaks of AO in ESB resulted in pronounced and sustained inflammation (*il-8, cc1, and cox-2*) involving many

novel molecules (Hepcidin) at the site of parasite attachment. Moreover, some of the genes related to pro-inflammation such as TNF-α and IL1β were down regulated, and this may be a result of a transient process. Therefore, this recent work highlighted the immediate local immune responses of ESB to natural AO infestation (Byadgi et al., 2019). However, further studies are needed to understand the time course expression of these upregulated immune genes under laboratory experimental infestation, in order to describe the physiological status of ESB during AO infestation and the subsequent recovery processes.

Therefore, the objectives of this study were to evaluate immune gene expression in gills and head kidney after AO infestation using RNA-seq, to evaluate the most differentially expressed genes in AO infested ESB and to investigate the chemokine *cc1* mRNA using *in-situ* hybridization (mRNA FISH) in order to survey the involvement of *cc1* against AO in the gills of ESB. Altogether, this study will provide a more comprehensive understanding of the roles of ESB immune genes during AO infestation and recovery.

2. Materials and methods

2.1 Ethics statement

All the experiments included in the present study have been carried out in the facilities (fish stabularium ID 5E7A0) of Department of Agricultural, Food, Environmental and Animal Sciences (University of Udine), as authorized by the Italian Ministry of Health (decree n 14/2018-UT, 12/11/2018). The animal care and protocols adopted adhere to the Directive 2010/63/EU of the European Parliament, implemented at a national level by the D.L. n. 26 of 4 March 2014.

2.2 Fish and parasite origin for experimental infestations

AO-naïve ESB (mean weight 14g) juveniles, sourced from an Italian Northeast hatchery, were acclimatized for two weeks in two separate recirculation systems, one for infection trial consisting of three 120 L fiberglass tanks (temperature 22.5±2°C, salinity 30±2‰ with natural photoperiod) and one structurally equal for control and with the same abiotic parameters. Fish was fed daily with commercial pellets and submitted to periodical veterinary control in order to assess their health status.

Trophonts obtained from natural infestations were collected and purified following the lab protocol (Beraldo et al., 2020; Byadgi et al., 2019) and subsequently early tomonts (before first division) were maintained *in vitro* at 16±0.5°C (hibernation status) until experimental infestation. Approximately 2 days before the experimental infestation the developmental process was reactivated by bringing them to 24°C to obtain viable dinospores.

2.3 Small scale infestation and RNA-sequencing

A dedicated small scale experimental infestation for RNA-seq was carried out in two 300L tanks (25‰ salinity and 24±2°C) at the University of Udine facilities, in one of which 5 ESB were infested by adding 4 dinospores/ml, whereas the other was left as control (5 uninfested ESB). After one week, infested and control ESB were euthanized (MS-222, 400 mg/L; E10521, Sigma-Aldrich) to collect gills and head kidney as study target organs. Total RNA from gills and anterior kidney was extracted using RNeasy Mini Kit (Qiagen, TX, USA).

2.4 Library construction and sequencing

Total RNA purity and degradation were checked on a 1% agarose gel. RNA integrity was assessed using the RNA Nano 6000 Assay Kit on the Bioanalyzer 2100 system (Agilent Technologies, CA, USA). Complementary DNA (cDNA) libraries were constructed using the TruSeq stranded mRNA Library Prep kit (Illumina®, USA). Libraries were sequenced (2×150bp) using the Illumina® platform NovaSeq 6000. Bbmap ver38.32 was used to remove remaining Illumina adapters from the sequencing reads. Bowtie2 (Langmead et al., 2012) (very sensitive settings) was used to align the cleaned reads against the *Dicentrarchus labrax* Transcriptome CDS (diclab1_cds.fasta; downloaded from NCBI) and unaligned reads were recovered in FASTQ format.

2.4.1 RNA seq data analysis

Raw data was analyzed using CLC Genomics Workbench v.12 (Qiagen Bioinformatics). Briefly, clean reads were obtained by removing low quality reads through trimming. High quality reads were aligned to the *D. labrax genome* downloaded from European seabass Genome Browser Gateway database (http://seabass.mpipz.mpg.de) with related annotations Mapping parameters: length fraction: 0.80, similarity fraction: 0.97, mismatch cost: 2, indels cost: 3.

2.4.2 Differentially expressed gene

Gene expression values were reported as TPM (Transcript per Million mapped reads). Genes that were identified as being differentially expressed met the following criteria: absolute fold change (FC) of >4, FDR *p-value* of <0.01 and Max group means of >10. Functional annotation of ESB genes were refreshed using Blast2Go (BioBam Bioinformatics S.L.).

2.5 AO experimental infestation and tissue collection for validation

Twenty-six fish/tank (mean weight 14 g) were stocked in three different tanks for infection and other three tanks for control in two independent recirculation systems (one for infested group, the other for the control group respectively) were used for the trial. Three days before infestation the water temperature was increased daily until 26±2°C and maintained for all experimental trial. Seventy Dinospores/ml were added to the designated "infested" tanks at a concentration of 3.5×10^6/tank. The time-course of infestation was monitored by the observation of clinical signs and by fresh gill microscopical examination. Fish became infested after 2 hours and at 2 days post-

infestation (dpi) the AO trophont burden in the gills was evident, with slight clinical symptoms. During the infestation, the maximum AO burden was observed at 10-12 dpi, thereafter fish started to recover even if positive for amyloodiniosis. Throughout this period, the total mortality was 18%. In the control group, fish were healthy, and no mortality was registered.

Differences in the expression levels of gill and head kidney innate immune genes at 2, 3, 5, 7 and 23 dpi were analysed using real-time PCR. Gills and head kidney were sampled (n=3/time point) as reported in paragraph 2.3 and preserved in RNA later until required.

2.6 Total RNA isolation and cDNA synthesis

Total RNA was isolated using TRIzol® reagent (Invitrogen Corp., Carlsbad, CA, USA, https://www.thermofisher.com/) according to manufacturer's instructions and the quantity and quality determined spectrophotometrically. The quality was also checked by running each sample on a 2% agarose gel and the RNA samples then stored at -80°C until required. For qPCR, 2 µg of total RNA was reverse-transcribed in a 20 µL reaction according to the manufacturer's protocol (iScript™ cDNA synthesis kit, Bio-Rad, http://www.bio-rad.com/).

2.7 Real-time PCR assays

The target and reference gene primers used in this study are detailed in Table 1. Amplifications were performed according to Byadgi et al., 2019 in a final volume of 10 µL. Each reaction contained 5 µL of IQ SYBR Green Supermix (Bio-Rad Laboratories, Hercules, CA, USA), 0.5 µL of each primer set (10 µM), 1 µL of template cDNA and 3 µL of DEPC-water. Real time PCR determinations were performed in triplicate in 96-well PCR plates and carried out in an CFX96 Touch Real-Time PCR Detection System (Bio-Rad Laboratories, Hercules, CA, USA) with an initial denaturation cycle of 95°C for 30 sec, followed by 40 cycles of 95°C for 5 sec and 60°C for 10 sec. Amplification was followed by a standard melting curve from 55°C to 95°C, in increments of 0.5°C for 5 sec at each step, to confirm that only one product was amplified and detected. Samples were run in parallel with three reference genes, beta-actin, hsp90 and L13a, for cDNA normalization (Mitter et al., 2009; Buonocore et al., 2017). Relative mRNA expression was calculated using the $2^{-\Delta\Delta Ct}$ method (Livak et al., 2001), normalizing with geometric average of three reference genes (β-actin, hsp90 and L13a) and relative to each control group.

2.8 *In situ* hybridization

The experimental infestation for the *in-situ* hybridization (ISH) was carried out in a 300L tank (25‰ and 24±2°C) at the University of Udine facilities, by adding dinospores (Dehority BA., 2003) to a final concentration of 4/ml. After one week, infested and control ESB juveniles were euthanized (MS-222, 400 mg/L; E10521, Sigma-Aldrich) to collect gills. Gills from AO-infested and control ESB juveniles were fixed in 4% paraformaldehyde in PBS (pH 7.4) (16005 & P5368, Sigma-Aldrich) overnight at 4°C, transferred to 70% ethanol and stored at -20°C. AO-infested and

control gills were also preserved in RNA later® (AM7021, Thermo Fisher Scientific) according to manufacturer's instructions and stored at -20°C.

The paraffin embedding of samples was performed at the Institute of Aquaculture, University of Stirling (Stirling, UK), and paraffin blocks stored at -20°C. Five µm sections were cut from the 4% paraformaldehyde-fixed, wax-embedded tissues, mounted onto Plus+ Frost positively charged microscope slides (MSS51012WH, Solmedia) and stored at -20°C.

2.8.1 Probes production. Total RNA was extracted from RNA later® preserved gill tissues using TRI Reagent (T9424, Sigma-Aldrich) as per manufacturer's instructions. The RNA was quantified using the Nanodrop (ND2000c, ThermoFisher Scientific) and the quality was assessed on a 1% agarose gel run with a 1Kb size marker (SM3014, Thermo Fisher Scientific). The gel was prepared with and run in 0.5× TAE buffer and contained ethidium bromide (EtBr) to a final concentration of 0.05µg/ml (E1510, Sigma-Aldrich). A 50µl, one-step reverse transcriptase PCR was performed with MyTaq One-Step RT-PCR kit (BIO-65408, BioLine) as per manufacturer's instructions, using 500ng total RNA and a final concentration of 400nM of each primer. The primers used were Chemo2FW and Chemo2RV (table 1b) which had been designed to amplify the immune-related transcript Chemokine CC1. The cycling profile was as follows: 45°C for 20 min, 95°C for 1 min, 40 cycles of 95°C for 10s, 60°C for 10s, 72°C for 30s, 72°C for 2 min and 10°C for 30 s. One point five µl of each PCR product was visualized on 1% agarose gel containing EtBr (0.05µg/ml) under UV light. The PCR products were purified using the QIAquick PCR Purification Kit (28104, QIAgen), as per manufacturer's instructions with minor modifications. Purified PCR products were then sent to GATC Biotech (www.eurofinsgenomics.eu/en/custom-dna-sequencing/gatc-services) for sequencing using their LightRun service. For the *in situ* hybridization step a second set of primers were produced to generate sense and anti-sense RNA probes by adding the T7 promotor sequence to the nucleotide sequences (Table 1b). The cycling protocol used was the same as that reported above. Digoxigenin (DIG)-labelling was performed using the DIG-RNA Labeling Kit (11 175 041 910, Sigma-Aldrich) following manufacturer′s instructions. DIG-labelled probes were aliquoted (1 µl) and stored at -70°C until required. To determine the yield of the DIG-labelled riboprobes a dot-blot analysis was carried out according to Sigma Aldrich protocol (DIG Application Manual for Nonradioactive In Situ Hybridisation, p59-64).

2.8.2 Fluorescent mRNA In-situ Hybridization (FISH)

Gill sections were dewaxed with xylene, rehydrated through a graded ethanol series, and then incubated in 2× Saline Sodium Citrate (SSC) (BP1325-1, ThermoFisher Scientific) for 1 min. Ten µg/ml Proteinase K (P2308, Sigma-Aldrich) was pipetted onto the tissue and digestion conducted, in a humidified box, at 37°C for 5 min. The reaction was stopped by immersing the slides in ice-

cold, 4% paraformaldehyde (in PBS) for 5 min, followed by two washes in PBS for 2 min each at RT. The slides were then dried as much as possible before a GeneFrame (AB-0578, Thermo Fisher Scientific) was placed over the sections to localise the reagents to the tissue. Slides were incubated with a Pre-hybridization solution (50% formamide, 20% 20× SSC and 30% nuclease-free ddH_2O) at 37°C for 10 min in a humidified box. The riboprobes (300-800ng/ml final concentration) were resuspended in the following hybridisation buffer: 50% (deionised) formamide (F9037, Sigma-Aldrich), 5× SSC, 10% dextran sulphate (D8906, Sigma-Aldrich), 5× Denhardt's solution (D2532, Sigma-Aldrich), 250 µg/ml yeast tRNA (15401-011, Invitrogen), 500 µg/µl herring sperm DNA (D1811, Promega) and 1% blocking solution (11585762001, Sigma-Aldrich). The hybridisation mix + riboprobes were heated at 80°C for 5 min and then cooled on ice before approximately 150 µl was pipetted onto the appropriate slide and covered with a GeneFrame coverslip. Hybridisation was performed overnight at 60°C in a humidified box. The following day, the coverslips and Geneframes were removed by rinsing in 2× SSC, slides were transferred into separate, individual 50 ml centrifuge tubes and washed twice in 2× SSC (30 min each) at RT on a rocking platform (Stuart Scientific). A high-stringency wash step was performed at 65°C for 30 min in 50% 2× SSC plus 50% deionised formamide, without agitation. This was followed by two washes in 2× SSC at 37°C for 10 min each on the rocking platform.

After post-hybridisation washes, transcripts were identified using the DIG nucleic acid detection kit (11175041910, Sigma-Aldrich) and DIG Wash and Block Buffer set (11585762001, Sigma-Aldrich), prepared as per the kit protocol. Sections were transferred to 1× Wash Buffer at RT for 5 min on rocking platform, followed by an incubation in 1× Blocking solution buffer at RT for 30 min with agitation. Sections were incubated for 2 h at RT with Anti-Digoxigenin-AP conjugate antibody (11175041910, Sigma-Aldrich) diluted 1:5,000 in 1× Blocking solution and then washed twice with 1× Wash buffer for 15 min at RT on rocking platform. Sections were dried as much as possible and equilibrated in 1× Detection buffer for 5 min at RT. Bound antibody was localized using Fast Red tablets dissolved in TRIS buffer (F4648, Sigma-Aldrich) as per manufacturer's instructions. 150 µl of Fast Red solution was added to each slide and incubated in the dark at RT in the humidified box (without agitation). Slides were monitored under a light microscope to prevent over-development and high background. As soon as a signal was detected or after a maximum of 30 min, the reaction was stopped by gently washing the slides with nuclease-free ddH_2O. Finally, the slides were dried and mounted with a coverslip using Vectamount AQ Aqueous Mounting Medium (H-5501, Vector Laboratories). Coverslip edges were sealed with clear nail varnish and the sections were incubated overnight to dry. Light and fluorescence microscopy images were captured using ArcturusXT™ Laser Capture Microdissection System (Nikon) microscope with an attached digital camera. Negative control slides, incubated with

hybridization mix only, were included (i.e. no riboprobes); a positive control slide consisted of a salmon louse (*Lepeophtheirus salmonis*) intestine section labelled with a trypsin antisense riboprobe.

2.9 Statistical analysis

Results were analysed using the SPSS16 (SPSS Inc., Chicago, IL, USA) statistical software. Data was tested for homogeneity of variance before ANOVA evaluation. Data distribution was determined using descriptive statistics. Data were given as mean ± standard deviation (SD). Statistical significances obtained from qRT-PCR analysis were subjected to one-way analysis of variance (one-way ANOVA) and compared using Duncan's multiple range test. Differences of means among the groups were considered statistically significant when $p<0.05$. Principal component analysis (PCA) and heat map was conducted using CLC Genomics Workbench v.12 (Qiagen Bioinformatics) on normalized RNA-seq data transcripts per million (TPM) of *D. labrax* gills and head kidney in response to infestation with *A. ocellatum*.

3. Results

3.1 Assembly and sequence description

Reads from control (n=3) and infested (n=5) tissues (gills and head kidney) were analyzed via Illumina sequencing in a paired-end 2x 150-nt run. This generated, on average, 23,321,464 raw reads per sample with a GC content of 52% (supplementary table 1). On average, 92.82% of the raw reads (21,646,982 reads) mapped to the European seabass (*D. labrax*) reference genome (supplementary table 2). The raw FastQ file has been deposited in the National Center for Biotechnology Information (NCBI) Sequence Read Archive (SRA) database under the accession number PRJNA588185.

3.2 PCA and heat map

PCA of the expression of all differentially expressed (DE) transcripts showed a clear clustering by tissue type and infestation group. This was as expected due to the specific expression pattern per tissue. Infestation with the parasite induced a shift in infested gills and the head kidney (supplementary Fig.1 & 2). Cluster analysis not only separated the different tissues from one another but also the gills from control-uninfested animals, suggesting that the most significant effects were taking place in the target tissue (supplementary Fig. 3). Cluster analysis also clearly separated the head kidney data from the control and infested groups (supplementary Fig 4).

3.3 Differentially expressed genes after *Amyloodinium ocellatum* infestation

Comparison of gene expression levels between AO infested and control groups revealed 1039 and 376 differentially expressed genes (DEG) in gills and head kidney respectively ($p < 0.01$). These included 679 upregulated genes and 360 downregulated genes in gills and 206 upregulated genes and 170 downregulated genes in head kidney (Fig. 1). The differentially expressed genes from

gills and head kidney were mainly annotated into biological process and molecular function. In gills, the highest number of DEG for the biological process (Fig 2a) were annotated to proteolysis (38), Oxidation-reduction process (30), immune response (18), proton transmembrane transport (11) and chemotaxis (9). The highest molecular processes (Fig 2b) in gills were annotated to protein binding (131), zinc ion binding (65), DNA binding transcription factor activity (25), calcium ion binding (25) and DNA binding (19). In head kidney (Fig 2c) the highest number of DEG for the biological processes were annotated to proteolysis (28), regulation of transcription DNA template (11), immune response (8), oxidation-reduction process (8), transmembrane transport (6) and protein phosphorylation (6). The highest molecular processes (Fig 2d) in head kidney were annotated to protein binding (39), calcium ion binding (19), ATP binding (18), zinc ion binding (13) and DNA binding (9).

In gills, among the immune response genes, the highest upregulation fold change (table 2) was recorded for c-c motif chemokine 21-like (581-fold), cc chemokine 1 (46-fold) and interleukin-12 subunit alpha-like (39 fold). On the contrary the major downregulated genes were tumor necrosis factor ligand superfamily member 12-like (-14-fold), somatomedin-b and thrombospondin type-1 (-1.70 fold), tumor necrosis factor ligand superfamily member 13b (-1.50 fold). Similarly, the top 3 upregulated and downregulated genes for proteolysis and protein binding are mentioned in (table 2). In head kidney among the immune response genes, the highest upregulated fold change (table 3) was recorded for cc chemokine 1 (22-fold), interleukin 10 precursor (22-fold) and c-x-c motif chemokine 10 precursor (13-fold). On the contrary the main downregulated genes were somatomedin-b and thrombospondin type-1 (-6-fold), tumor necrosis factor ligand superfamily member 10-like (-4-fold) and tumor necrosis factor alpha (-2.5-fold). Similarly, the top 3 upregulated and downregulated genes in head kidney for proteolysis and protein binding are mentioned in table 5.

Based on the DEG with highest fold change, the lists of the top 20 genes that were up-or down regulated in the gills (supplementary table 3) and head kidney (supplementary table 4) were observed in non-infested gills and head kidney, respectively. In gills, among the top 20, three highly up-regulated immune genes were perforin 1 like (1806.91-fold), gtpase (800.18-fold), and receptor transporting protein 3 (675.40-fold). Similarly, the top 3 downregulated genes were protein-glutamine gamma-glutamyl transferase 5 isoform 1 (-2151.91-fold), Caspase 1 (-169.66-fold), and gastrin cholecystokinin-like peptide-like (-161.77-fold). In head kidney (table 7), three of the most highly up-regulated immune genes were interferon inducible Mx protein (4869.73-fold), tubulin alpha1 chain (872.52-fold) and receptor transporting protein 3 (687.97-fold). Similarly, the top 3 downregulated immune genes were arylamine n- pineal gland isozyme nat-10-

like (-6427.56-fold), dual specificity tyrosine-phosphorylation-regulated kinase 1a-like (-787.65-fold) and carboxypeptidase b (-272.84-fold).

3.4 Validation of RNA-seq by qPCR and *in situ* hybridization

Throughout the time course infestation trial, the total mortality was 18%. In the control group, fish were not infested, and no mortality was registered. Expression changes of innate immune genes in gills and head kidney were analyzed at 2, 3, 5, 7 and 23 dpi. In gills (Fig 3), among the pro-inflammatory molecules, CC1 (2-fold) and IL-8 (2-fold) started to peak at 5 dpi and were significantly higher at 7 dpi while COX-2 was unaffected during the course of infestation. Hepcidin (4.2-fold) and CLA (2-fold) were significantly higher at 2 and 3 dpi and declined at 5 and 7 dpi, while CASP9 was not affected post-infestation. Immunoglobulins IgM and IgT were unaffected in gills during the course of infestation until 7dpi (Fig 5 a & b).

In head kidney (Fig 4), CC1 (2-fold) was significantly higher at 2 dpi and 3 dpi but decreased thereafter. However, IL-8 and COX-2 were not affected by the infestation. Hepcidin (40-fold) peaked at 7 dpi while CASP9 (2-fold) peaked at 5 dpi. CLA was not affected by infestation. IgM (6.2-fold) peaked at 3 dpi and declined thereafter but IgT did not show significant changes in expression until 7dpi (Fig 5 c & d).

During the recovery phase (23 dpi) the expression of CC1 (18-fold), hepcidin (20-fold) and IgM (9-fold) in the gills (Fig 6a), was significantly increased compared to other genes while in head kidney (Fig 6b), IgM (10-fold) and IgT (6 fold) were higher compared to control.

Through *in situ* hybridization it was possible to observe that in the uninfested control fish the gene signal CC1was evident in the gill associated lymphoid tissue (GIALT) (Fig. 7 a,b), in the lumen of the central venous sinus and in the capillaries of the apical portion of the primary lamellae (data not shown). In the infested fish, a higher abundance of CC1 positive leukocytes was observed in the hyperplastic regions of the secondary lamellae (Fig. 8 a-d) and in the vessel wall (diapedesis) of the central venous sinus of primary lamellae (Fig. 8 a-d). In general, the signal intensity was lower in uninfested control fish, whereas in the infested subjects the signal was visibly higher. In the gills of infested fish, no positive signal was detected near the trophont adhesion sites (Fig. 12 c & d). In the negative controls (no riboprobes) and in the samples hybridised with Chemokine CC1 sense probe, no positive signal was detected in the examined gill tissues (Fig. 7 c-f; Fig. 9 a-d). Sea louse (*L. salmonis*) intestine labelled with Trypsin antisense probe (Fig. 9e & f) represented a reference positive control.

4. Discussion

The purpose of the present investigation is to provide general insights on how host and parasite interact. In our previous study dealing with ESB response after natural AO infection (Byadgi et

al., 2019) we observed that none out of four genes codifying for molecules related to adaptive immunity (mhc i, mhc ii and igm) show upregulation in gills and head kidney. This phenomenon could be due to the nature (characteristics) of the host species and to the infection dynamics (intended as mode of response in relation to the days post infection). Consequently, to the host interaction with the parasite there was a pronounced and sustained inflammation (il-8, chemokine cc1, cox-2) that brought many novel molecules (Hepcidin) to the site of parasite adhesion. Therefore, from the present study and from the previous study as well it can be confirmed that local innate immunity plays a major role during AO infection in ESB. During experimental infection, RNA-seq was analysed at one time point during initial stage of infection and most of the DEG recorded are therefore related to innate immunity which could be consequent to AO infection. Based on the information we obtained from these two studies we can speculate that innate immune responses with CC1, antimicrobial peptides, IL-8, COX-2 dominate the response in ESB after AO infection, although we cannot exclude the involvement of specific antibodies and lymphocytes at the systemic level.

We conducted the present study under "controlled infestation conditions" in order to understand the time course expression of upregulated immune genes, the physiological status of the host, and to determine their potential as functional markers in the ESB infested by AO. This is the first time that this interaction has been studied for ESB and the present study was performed to extend our understanding on this matter. In our previous study, we used Real-time quantitative PCR to investigate immune gene expression and demonstrated their importance when fish responded to AO exposure (Byadgi et al., 2019). However, the genes previously investigated are likely to account for only a small proportion of the immune processes occurring in such tissues. The RNA-seq analysis presented here aims to fill the gaps in our understanding of these pivotal immune processes post-AO infestation in ESB.

We found more differentially expressed genes in gills (1039) than in head kidney (376) after AO infestation. This is not that surprising since the gills are the main target tissue of AO infestation and the parasite attachment in ESB is mostly restricted to this organ. Additionally, the distinctive clinical sign of the disease, i.e. anaemia, is attributable to the alteration of the gill physiology induced by the parasite. Furthermore, kidney analysis revealed 170 down-regulated genes, an interesting result that can be attributed to the common lympho-haematopoietic functions and to the cellular depletion as similarly observed in the spleen and kidney of turbot (*S. maximus*) infested by *Enteromyxum scophthalmi* (Bermúdez et al., 2010; Haase et al., 2014).

Based on the highest fold change observed, our findings from RNA-seq in gills suggest that perforin might play significant roles in the immune system and in the ESB immune defense against AO. Meantime, the differential expression dynamics seem to imply possible different cellular

locations or functional differences. Perforin was first characterized as a lytic pore-forming protein isolated from cytotoxic T lymphocytes (CTLs) (Podack et al., 1985). In humans and mice perforin is a single-copy gene and its immunological function has been well studied. However, unlike humans and mice, there is more than one perforin gene in fish genomes (Toda et al., 2011; Varela et al., 2016), although only one isoform has been reported, in teleosts, to date (Hwang et al., 2004; Athanasopoulou et al., 2009; Jung et al., 2014; Taylor et al., 2016).

In head kidney several genes related to the interferon-mediated immune response and the promyelocytic leukemia protein (PML) gene were upregulated. The PML gene positively regulates the type I interferon response by promoting transcription of IFN-stimulated genes (ISGs) (Kim et al., 2014). Also, during AO infestation in head kidney, we observed genes related to IFN signalling, with an increased expression of IFN-gamma showed the highest number of DE genes. Overall, these results point towards a response mediated by both type II IFNs, as observed in early stages of several protozoan infestations occurring in mammals (Beiting et al., 2014). In teleosts parasitized by amoebae and myxozoan parasite, the IFN-mediated immune response was shown to play a major role, with implications for fish resistance or susceptibility to the disease (Young et al., 2008; Davey et al., 2011; Bjork et al., 2014). It was observed that in turbot facing advanced stages of enteromyxosis, IFN-related genes were markedly downregulated, suggesting a differential immune response during the different phases of infestation to enteromyxosis in turbot (Robledo et al., 2014). Having observed the upregulation of several interferon genes during AO infestation, we could speculate that IFN expression might depend on the stage of infestation or on the localization of the parasite during the infestation.

In the RNA-seq data, we found four chemokines (*cc21*, *cc1*, *cc10*, and *cc19)* significantly upregulated in infested gills and head kidney compared with control. These results suggest that more immune cells were recruited in the infested sites. A previous study demonstrated that IL-8 produced in human intestinal mucosa during infestation was capable of recruiting blood monocytes and maintaining the macrophage population in the mucosa (Smythies et al., 2006). In rainbow trout, IL-8 had the analogous capability of attracting monocyte-macrophage cells during infestation (Montero et al., 2008). IL8 and CXCR1 correspond to chemokine (CK) and chemokine receptors (CR) in mammals, while other CKs and CRs have no ligand-receptor correlation. In this study, the fold-change of the up-regulation of *cc21* was extremely high (581-fold). Also, CCL19 in this study was 11-fold up regulated in the head kidney. CCL19 and CCL21 are homeostatic chemokines, which play an important role in T and B cell trafficking and migration to peripheral lymphoid tissues in mammals (Choi et al., 2003), whereas in turbot CCL19 was reported to attract head kidney leukocytes and augment host immune defense (Chen et al., 2013). CXCL9, CXCL10 and CXCL11 are known in mammals as a group of interferon inducible chemo attractants

recruiting activated CD4þ Th1 cells, CD8þ T cells and NK cells (Liu et al., 2007; Cheng et al., 2011). Therefore, the immune response induced by all upregulated chemokines probably leads to the enhanced resistance against AO pathogen in ESB. Hence, further studies should be directed towards understanding the biological activity and functionality of ESB chemokines during amyloodiniosis.

In gills and head kidney among the proteolysis category, the most common upregulated gene was matrix metalloproteinase, after AO infestation. Matrix metalloproteinases (MMPs) have important functions in extracellular matrix (ECM) degradation and tissue repair (Page-McCaw et al., 2007). Mmp-9 has been found to contribute to leukocyte migration, thus participating in mammalian inflammation and immunity (Van den Steen et al., 2007; Greenlee et al., 2007). Mmp-9 in zebrafish (*Danio rerio*) is expressed notably in the head-kidney and in peritoneal and peripheral blood leukocytes upon infestation, indicating its role in immune responses (Chadzinska et al., 2008). In *Mycobacterium marinum* infested zebrafish, Mmp-9 was found to enhance recruitment of macrophages and to contribute to granuloma formation and bacterial growth (Volkman et al., 2010). Therefore, our findings suggest that Mmp is a protective molecule against AO in ESB via a proteolytic role.

In gills and head kidney of ESB after AO infestation, the RNA-seq data revealed that the TNF-α and TNF superfamily genes were downregulated. In our previous study, we similarly observed that there was a lack of *il-1β* and *tnf-α* expression in gills (Byadgi et al., 2019). Toxins or enzymes released by the parasites might have damaged the leucopoietic system resulting in reduction in the expression of most of the immune-related genes, including tnf-α (Kar et al., 2016). However, functionally assessed to have pro-inflammatory activity in fish, *il-1β* and *tnf-α* are often co-expressed with other macrophage-derived inflammatory mediators such as *il-8*, *cox-2*, and *inos* in parasitic and bacterial infestations (Harun et al., 2011; Bruijn et al., 2012; Oladiran et al., 2011; Alvarez-Pellitero et al., 2008; Covello et al., 2009). Some cytokine genes were mainly down regulated including TNF-α, an important proinflammatory cytokine in fish (Sigh et al., 2004). Although this cytokine may play a role in the initiation of the early immune response and has multiple effects on gene expression during inflammation (Dinarello et al., 2009), IL-1β expression was likely suppressed in rainbow trout in late stages of the infestation. Depression of pro-inflammatory cytokine production in rainbow trout macrophages infested with *Renibacterium salmoninarum* was previously demonstrated (Grayson et al., 2002). In addition, TNF-α, considered as an important component in the inflammatory response in fish (Secombes et al., 2001) and activated in rainbow trout after i.p. injection of live theronts of *I. multifiliis* (Jørgensen et al., 2008), was not triggered or up regulated by infestation. In *Gymnocypris przewalskii*, *I. multifiliis* infestation enhanced TNF synthesis because of the up regulation of TLR genes (Tian et al., 2017).

Therefore, in AO infested ESB the lack of evidence for TNF-α and IL-1β expression at the time point under study could be due to the transient fluctuation of expression of these genes throughout the infestation.

In ESB after AO infestation, we observed the downregulation of complement *c3* and *c9 genes*, which may be associated with susceptibility to AO and mortality in ESB. The complement system (Wood P., 2011) is an essential part of the innate immunity (Holland et al., 2002) in alerting the host to the presence of potential pathogens (Boshra et al., 2006) and plays a crucial role in the response or resistance against Ich (Buchmann et al., 1999; Buchmann et al., 2001; Heidarieh et al., 2015). In rainbow trout, complement factor C9 played a role in the skin and gills during parasite-host interaction (Sigh et al., 2004; Jørgensen et al., 2008; Olsen et al., 2011) and against the bacterial pathogen *Yersinia ruckeri* (Chettri et al., 2012). Although other studies indicated high expression of *c3* in the liver, head kidney, skin, gill and spleen of infested individuals, our results indicated its down-regulation (Heidarieh et al., 2015; Sigh et al., 2004; Jørgensen et al., 2008; Olsen et al., 2011). Altogether, it is evident that the complement system plays a much more important role in infested gills sites where it comes into direct contact with AO. It is still not known whether and how complement components affect the AO infestation outcome in ESB but it can be hypothesized that AO also evolved with a strategy to evade or counteract the complement system of ESB.

Therefore, from the present study and from the previous study as well (Byadgi et al., 2019), it can be confirmed that local innate immunity plays a major role during AO infestation in ESB. During experimental infestation, RNA-seq was analysed at onetime point during initial stage of infestation and most of the DEG recorded are therefore related to innate immunity which could be consequent to AO infestation. Based on the information we have from the two studies we can speculate that innate immune responses with CC1, antimicrobial peptides, IL-8 dominate the response in ESB after AO infestation at the early phase, although we cannot exclude the involvement of specific antibodies and lymphocytes which requires further studies. The fact that the "post infestation course" in AO episodes (either natural or experimentally induced) is usually rather rapid, therefore we can reasonably speculate that the genes of innate immunity are more expressed than those of specific immunity.

RNA-seq data validation

In our previous study, we observed that *cc1* expression was upregulated in AO infested gills, indicating that a pro-inflammatory stimulus was activated by the host response *versus* the parasite (Byadgi et al., 2019). In our present investigation, gills and head kidney showed a high fold change of *cc1* post-AO infestation. Interestingly, chemokine expression increases when there is tissue damage and most chemokines are recognized as pro-inflammatory factors; they have been shown

to exert regulatory functions in a wide range of pathological and physiological contexts, such as hypersensitivity reactions, infestation, angiogenesis, inflammation, tumor growth and haematopoietic tissues development (Suresh et al., 2006; Nibbs et al., 2013; Stone et al., 2017). Given their critical role in inflammation, many chemokines and chemokine receptors have been identified as potential therapeutic targets in a wide range of inflammatory diseases (Proudfoot et al., 2002). Chemokines (CKs) known as chemotactic cytokines recruit immune cells into the sites of injury or infestation in acute inflammation. They act via binding to specific G protein-coupled receptors on target cells, which orchestrate immune cell migration and positioning at the organismic level in the host. The expression of *cc1* and *il-8* in infested gill tissues on day 5 indicates that the genes were expressed during the inflammation process. In rainbow trout (*Oncorhynchus mykiss*), CC chemokines were up regulated in liver after challenge with haemorrhagic septicaemia virus (VHSV) and infectious pancreatic necrosis virus (IPNV) (Montero et al., 2008). Up-regulation of CC chemokines was detected in spleen (15-fold) and liver (29-fold) of miiuy croaker (*Miichthys miiuy*) infected by *Vibrio anguillarum* (Cheng et al., 2011). Significant up-regulation of *cc1* in all tissues of *Lates calcarifer* infested by *C. irritans* was also reported (Mohd-Shaharuddin eta l., 2013). Although the regulation of *cc1* genes in affected host organs has previously been reported (Byadgi et al., 2019), the present study demonstrated that gills (harbouring a relevant parasite load) responded significantly stronger compared to head kidney. Also, the time dependent high up-regulation of *cc1* and *il-8* in ESB post AO infestation may indicate that *cc1* and *il-8* have a prominent role in the response against *AO*.

Another interesting result observed after AO infestation in ESB, was the time related change in Hepcidin expression in both gills and head kidney. In gills, it was significantly increased at 2 dpi but in head kidney, it was highest at 7dpi. Hepcidin transcription was described as increased in anaemic fish due to *Photobacterium damselae* infection (Rodrigues et al., 2006). Elevation of hepcidin (42-fold) in the liver of rainbow trout (*Oncorhynchus mykiss*) infected by *Y. ruckeri* has also been reported (Raida et al., 2009). Up-regulated expression of the hepcidin gene at days 3 and 10 post *C. irritans* infestation was found in *Lates calcarifer* liver, kidney, gill and spleen tissues (Mohd-Shaharuddin eta l., 2013). Time-dependent changes in hepcidin expression were recorded in *Labeo rohita* at 3 dpi with *Argulus siamensis.* These were significantly high in liver and kidney tissues but negligible in skin (Kar et al., 2015). In healthy organisms, iron concentration is maintained at a stable level in plasma, and this element is stored in hepatocytes and splenic/hepatic macrophages at constant levels, despite unstable absorption of iron from the diet (Hermenean et al., 2017). It has been reported that hepcidin-mediated low serum iron level functions as a host defense mechanism that evolved to restrict iron availability for pathogen growth and development

(Drakesmith et al., 2012; Ganz et al., 2015). This validates the results obtained from our previous study on natural infestation of ESB with AO and suggests that hepcidin could possibly be considered a relevant immune marker in ESB, providing a protective effect in the fish when highly expressed.

In our previous study, the lower level or no expression of *igm* in infected samples indicated that the parasite toxins might negatively influence the systemic specific immune response (like production of igm) (Covello et al., 2009) or alternatively that the disease reached its onset very rapidly and the individuals did not have enough time to activate a specific humoral response. Therefore, in the present study we evaluated time course Igm and Igt expression and similar results were observed until 7dpi but at 23 dpi indicated that in gills and head kidney there was an upregulation of igm and igt. There are few reports on igm/igt expression in gills and skin after parasite infestation (Zhang et al., 2010; Olsen et al., 2011; Xu et al., 2013). Further research should be directed to evaluate the immune response in skin to complete the evidence that mucosal immune response plays an important role during AO infestation in ESB.

In this study, a fluorescent mRNA *in situ* hybridization (FISH) protocol was developed to investigate the host-parasite interactions by determining the presence or absence of Chemokine CC1 mRNA sequences in affected tissues. The fluorescent signal was localized within specific cells allowing a semi-quantitative estimation of the level of occurrence/expression. Based on our knowledge, there is no documented information about previous FISH based approaches in ESB gills infested by *A. ocellatum*. In uninfested fish, a faint hybridization signal was detected in the GIALT, in the lumen of the central venous sinus and in the capillaries of the apical portion of the primary lamellae. On the other hand, Chemokine CC1 signal was more evident in infested gill tissue, with positive cells detected in the hyperplastic areas of the secondary lamellae and in the vessel wall of the central venous sinus of the primary lamellae. Interestingly, a positive signal was also detected in the cytoplasm of some trophonts, potentially suggesting the "phagotrophic" nature of the dinoflagellate as previously speculated (Lom et al., 2002) and also observed in our previous immunohistochemical survey (Byadgi et al., 2019). On the other hand, no positive signal was detected in the tissue areas close to anchored parasites. A possible explanation for the absence of positive cells in those areas may be due to evasive mechanisms adopted by the protozoan to avoid detection and defense by the host immune system, as documented for other fish parasites (Buchmann et al., 2002; Sitjà-Bobadilla 2008; Kumar et al., 2013). The results reported here also support the observed differential expression of Chemokine CC1 transcript between uninfested and infested European sea bass and provide a better understanding of the pattern of localisation of

leukocyte populations in ESB gills. These results suggest that *cc1* plays an important role against AO attachment and pathogenicity.

5. Conclusions

In this study, the immune mechanisms in ESB gills and head kidney after infestation by AO, indicated partial overview of the mucosal response. Gills showed a higher number of DEG compared to head kidney, indicating the importance of the mucosal immune response at the site of AO attachment. Several immune genes were altered after AO infestation, such as chemokine *cc1*; multiple genes of the interferon-mediated immune response were upregulated. This points to a recruitment of immune cells towards the site of AO attachment in ESB gills. Moreover, the downregulation of tumor necrosis factors and complement factors in ESB indicated the potential temporary nature of TNF-α expression and of the invasion mechanisms triggered by AO to counteract the ESB. The upregulation of chemokines was also validated by qPCR and *in situ* hybridization, specific for chemokine CC1, evidencing that chemokines play an important role in the local immune response during AO infestation in ESB. Therefore, the molecular modifications at the base of host and pathogen interaction identified here provide a basis to better understand processes that may influence ESB immune performance during AO infestation.

Conflict of Interests

The authors declare that there is no conflict of interest.

Acknowledgements

The present study was performed under the European Union support: Horizon 2020 project Parafishcontrol (grant agreement No. 634429) and Aquaexcel research and innovation programme (grant agreement No. 652831). The output reflects only the authors view, and the European Union cannot be held responsible for any use that may be made of the information contained herein. The authors wish to thanks the technicians Pierluigi Bagatella and Carla Calligaro for their lab assistance and Prof. Emilio Tibaldi for his help during the study. Further thanks to Dr. Sean J. Monaghan and Dr. John B. Taggart, from University of Stirling for their assistance during the study.

References

Allardo-Escárate, C., Valenzuela-Muñoz, V., Nuñez-Acuña, G.,2014. RNA-Seq analysis using de novo Transcriptome assembly as a reference for the salmon louse *Caligus rogercresseyi.* PLoS ONE 9, e92239.

Alvarez-Pellitero, A., 2008. Fish immunity and parasite infections: from innate immunity to immunoprophylactic prospects, Vet. Immunol. Immunopathol. 126, 171–198.

Alvarez-Pellitero, P., Sitjà-Bobadilla, A., Franco-Sierra, A., 1993. Protozoan parasites of wild and cultured sea bass, *Dicentrarchus labrax* (L.), from the Mediterranean area. Aquacult. Fish. Manage. 24 (1), 101-108.

Athanasopoulou, S., Marioli, D., Mikrou, A., Papanastasiou, A.D., Zarkadis, I.K., 2009. Cloning and characterization of the trout perforin. Fish Shellfish Immunol. 26(6), 908–12.

Beiting, D.P., 2014. Protozoan parasites and type I interferons: a cold case reopened. Trends Parasitol. 30, 491–498.

Benetti, D.D., Orhun, M.R., Sardenberg, B., O'Hanlon, B., Welch, A., Hoenig, R., Zink, I., Rivera, J.A., Denlinger, B., Bacoat, D., Palmer, K., Cavalin, F., 2008. Advances in Hatchery and Grow-out Technology of Cobia *Rachycentron canadum* (Linnaeus). Aquac. Res. 39, 701-711.

Beraldo, P., Massimo, M., Galeotti, M., 2020. SOP for Amyloodinium ocellatum. In Fish Parasites: A Handbook of Protocols for Their Isolation, Culture and Transmission; Sitjà-Bobadilla, A., Bron, J.E., Wiegertjes, G.F., Piazzon, M.C., Eds.; Sheffield: 5M publishing (in press).

Bermúdez, R., Losada, A.P., Vázquez, S., Redondo, M.J., Álvarez-Pellitero, P., Quiroga, M.I., 2010. Light and electron microscopic studies on turbot *Psetta maxima* infected with *Enteromyxum scophthalmi*: histopathology of turbot enteromyxosis. Dis. Aquat. Organ. 89 (3), 209-21.

Bjork, S.J., Zhang, Y.A., Hurst, C.N., Alonso-Naveiro, M.E., Alexander, J.D., Sunyer, J.O., Bartholomew, J.L., 2014. Defenses of susceptible and resistant Chinook salmon (*Oncorhynchus tshawytscha*) against the myxozoan parasite *Ceratomyxa shasta*. Fish Shellfish Immunol. 37, 87–95.

Boshra, H., Li, J., Sunyer, J.O., 2006. Recent advances on the complement system of teleost fish. Fish. Shellfish. Immunol. 20(2), 239–62.

Brown, E.M., 1994. On *Oodinium ocellatum* Brown, a parasitic dinoflagellate causing epidemic disease in marine fish. Proc. Zool. Soc. Lond. 583-607.

Bruijn. I.D., Belmonte, R., Anderson, V.L., Saraiva, M., Wang, T., Van West, P., Secombes C.J., 2012. Immune gene expression in trout cell lines infected with the fish pathogenic oomycete *Saprolegnia parasitica*, Dev. Comp. Immunol. 38, 44–54.

Buchmann, K., Lindenstrøm, T., 2002. Interactions between monogenean parasites and their fish hosts. Int. J. Parasitol. 32, 309–319.

Buchmann, K., Lindenstrøm, T., Sigh, J., 1999. Partial cross protection against *Ichthyophthirius multifiliis* in *Gyrodactylus derjavini* immunized rainbow trout. J Helminthol. 73(03), 189–95.

Buchmann, K., Sigh, J., Nielsen, C.V., Dalgaard, M., 2001. Host responses against the fish parasitizing ciliate *Ichthyophthirius multifiliis*. Vet Parasitol. 100, 105–16.

Buonocore, F., Stocchi, V., Nunez-Ortiz, N. Randelli, E., Gerdol, M., Pallavicini, A., Facchiano, A., Bernini, C., Guerra, L., Scapigliati, G., Picchietti, S., 2017. Immunoglobulin T from sea bass (*Dicentrarchus labrax* L.): molecular characterization, tissue localization and expression after nodavirus infection. BMC Molecular Biol. 18(1), 8.

Byadgi, O., Beraldo, P., Volpatti, D., Massimo, M., Bulfon, C., Galeotti, M., 2019. Expression of infection-related immune response in European sea bass (*Dicentrarchus labrax*) during a natural outbreak from a unique dinoflagellate *Amyloodinium ocellatum*. Fish Shellfish Immunol. 84, 62-72.

Cecchini, S., Saroglia, M., Terova, G., Albanesi, F., 2001. Detection of antibody response against *Amyloodinium ocellatum* (Brown, 1931) in serum of naturally infected European sea bass by an enzyme-linked immunosorbent assay (ELISA). Bull. Eur. Ass. Fish Pathol. 21, 104-108.

Chadzinska, M.P., Baginski, E., Kolaczkowska, H.F.J., Savelkoul, B.M.L., Verburg-van Kemenade., 2008. Expression profiles of matrix metalloproteinase 9 in teleost fish provide evidence for its active role in initiation and resolution of inflammation. Immunol. 125, 601-610.

Chen, C., Hu Y.H., Xiao, Z.Z., Sun, L., 2013. SmCCL19, a CC chemokine of turbot *Scophthalmus maximus*, induces leukocyte trafficking and promotes anti-viral and anti-bacterial defense Fish Shellfish Immunol. 35, 1677-1682.

677 Cheng, Y.Z., Wang R.X., Xu T.J., 2011. Molecular cloning, characterization and expression
678 analysis of a miiuy croaker (*Miichthys miiuy*) CXC chemokine gene resembling the
679 CXCL9/CXCL10/CXCL11. Fish. Shellfish Immunol. 31, 439-445.

680 Chettri, J.K., Raida, M.K., Kania, P.W., Buchmann, K., 2012. Differential immune response of
681 rainbow trout (*Oncorhynchus mykiss*) at early developmental stages (larvae and fry) against
682 the bacterial pathogen *Yersinia ruckeri*. Dev comp immunol. 36(2), 463–74.

683 Choi, Y. K., Fallert B.A., Murphey-Corb M.A., Reinhart, T.A., 2003. Simian immunodeficiency
684 virus dramatically alters expression of homeostatic chemokines and dendritic cell markers
685 during infection in-vivo. Blood. 101,1684–1691.

686 Cobb, C.S., Levy, M.G., Noga, E.J., 1998. Acquired immunity to amyloodiniosis is associated
687 with an antibody response. Dis. Aquat.Org. 34, 125-133.

688 Cordero, H., Laura, T., Guzman-Villanueva., Chaves-Pozo, E., Arizcun., M., Ascencio-Valle., F.,
689 Cuesta., A., Esteban, M.A., 2016. Comparative ontogenetic development of two marine
690 teleosts, gilthead seabream and European sea bass: New insights into nutrition and
691 immunity. Dev. Comp. Immunol. 65, 1-7.

692 Covello, J.M., Bird, S., Morrison, R N., Battaglene, S.C., Secombes, C.J., Nowak, B.F., 2009.
693 Cloning and expression analysis of three striped trumpeter (*Latris lineata*) pro-inflammatory
694 cytokines, TNF-α, IL-1β and IL-8, in response to infection by the ectoparasitic,
695 *Chondracanthus goldsmidi*, Fish Shellfish Immunol. 26, 773–786.

696 Covello, J.M., Bird, S., Morrison, R.N., Battaglene, S.C., Secombes, C.J., Nowak BF., 2009.
697 Cloning and expression analysis of three striped trumpeter (Latris lineata) pro-inflammatory
698 cytokines, TNF-α, IL-1β and IL-8, in response to infection by the ectoparasitic,
699 Chondracanthus goldsmidi. Fish Shellfish Immunol. 26, 773-786.

700 Cruz-Lacierda, E.R., Maeno, Y., Pineda, A.J.T., Matey, V.E., 2004. Mass mortality of hatchery-
701 reared milkfish (*Chanos chanos*) and mangrove red snapper (*Lutjanus argentimaculatus*)
702 caused by *Amyloodinium ocellatum* (Dinoflagellida). Aquacult, 236, 85-94.

703 Davey, G.C., Calduch-Giner, J.A., Houeix, B., Talbot, A., Sitjà-Bobadilla, A., Prunet, P., Pérez
704 Sánchez, J., Cairns, M.T., 2011. Molecular profiling of the gilthead sea bream (*Sparus*
705 *aurata* L.) response to chronic exposure to the myxosporeans parasite *Enteromyxum leei*.
706 Mol. Immunol. 48, 2102–2112.

707 Dehority, B.A., 2003. Rumen microbiology. Nottingham University Press: pp. 349-350.

Dequito, A.Q.D., Cruz-Lacierda, E.R., Corre Jr., V.L., 2015. A Case Study on the Environmental Features Associated with *Amyloodinium ocellatum* (Dinoflagellida) Occurrences in a Milkfish (*Chanos chanos*) Hatchery. AACL Bioflux. 8(3), 390–397.

Dinarello, C.A., 2009. Immunological and inflammatory functions of the interleukin-1 family. Annu Rev Immunol. 27, 519–50.

Drakesmith, H., Prentice, A.M., 2012. Hepcidin and the iron-infection Axis**.** Science. 338, 768-772.

Fioravanti, M.L., Caffara, M., Florio, D., Gustinelli, A., Marcer, F., 2006. A parasitological survey of European sea bass (*Dicentrarchus labrax*) and gilthead sea bream (*Sparus aurata*) cultured in Italy. Vet. Res. Commun. 30, 249-252.

Ganz, T., Nemeth., E., 2015. Iron homeostasis in host defense and inflammation. Nat. Rev. Immunol. 15, 500-510.

Gómez, F., Gast, R.J., 2018. Dinoflagellates *Amyloodinium* and *Ichthyodinium* (Dinophyceae), parasites of marine fishes in the South Atlantic Ocean. Dis. Aquat. Organ, 131, 29-37.

Grayson, T.H., Cooper, L.F., Wrathmell, A.B., Roper, J., Evenden, A.J., Gilpin, M.L., 2002. Host responses to *Renibacterium salmoninarum* and specific components of the pathogen reveal the mechanisms of immune suppression and activation. Immunology. 106, 273–83.

Greenlee, K.J., Werb, Z, Kheradmand, F., 2007. Matrix metalloproteinases in lung: multiple, multifarious, and multifaceted. Physiol. Rev. 87, 69-98.

Haase, D., Rieger, J.K., Witten, A., Stoll, M., Bornberg-Bauer, E., Kalbe, M., Reusch, T.B.H., 2014. Specific gene expression responses to parasite genotypes reveal redundancy of innate immunity in vertebrates. PLoS ONE. 9: e108001.

Haase, D., Rieger, J.K., Witten, A., Stoll, M., Bornberg-Bauer, E., Kalbe, M., Reusch, T.B.H., 2016. Immunity comes first: The effect of parasite genotypes on adaptive immunity and immunization in three-spined sticklebacks. Dev. Comp. Immunol. 54, 137–144.

Harun, N.O., Wang, T., Secombes, C.J., 2011. Gene expression profiling in naïve and vaccinated rainbow trout after *Yersinia ruckeri* infection: Insights into the mechanisms of protection seen in vaccinated fish. Vaccine. 29 (26), 4388-99.

Heidarieh, M., Diallo, A., Moodi, S., Taghinejad, V., Akbari, M., Monfaredan, A., 2015. Gene expression analysis in rainbow trout (*Oncorhynchus mykiss*) skin: immunological responses to radiovaccine against *Ichthyophthirius multifiliis*. Revue Med Vet. 166(7–8), 233–42.

Hermenean, A., Gheorgiu, G., Stan, M.S., Herman, H., Onita, B., Ardelean, D.P., Ardelean, A., Braun, M., Zsuga, M., Keki, S., Costache, M., 2017. Dinischiotu Biochemical, Histopathological and Molecular Responses in Gills of Leuciscus cephalus Exposed to Metals. Arch. Environ. Contam. Toxicol. 73, 607-618.

Holland, M.C.H., Lambris, J.D., 2002. The complement system in teleosts. Fish Shellfish Immunol. 12 (5), 399–420.

Hu, Y., Li, A.; Xu, Y., Jiang, B., Lu, G., Luo, X., 2017. Transcriptomic variation of locally-infected skin of *Epinephelus coioides* reveals the mucosal immune mechanism against *Cryptocaryon irritans*. Fish Shellfish Immunol. 66, 398–410.

Hwang, J.Y., Ohira, T., Hirono, I., Aoki, T., 2004. A pore-forming protein, perforin, from a non mammalian organism, Japanese flounder, *Paralichthys olivaceus*. Immunogenetics. 56(5), 360–7.

Jørgensen, L.V.G., Nemli, E., Heinecke, R.D., Raida, M.K., Buchmann, K., 2008. Immune-relevant genes expressed in rainbow trout following immunisation with a live vaccine against *Ichthyophthirius multifiliis*. Dis Aquat Organ. 80(3), 189–97.

Jung, M.H., Nikapitiya, C., Song, J.Y., Lee, J.H., Lee, J., Oh, M.J., Jung, S.J., 2014. Gene expression of pro- and anti-apoptotic proteins in rock bream (*Oplegnathus fasciatus*) infected with megalocytivirus (family Iridoviridae). Fish Shellfish Immunol. 37(1), 122–30.

Kar, B. Mohanty, J., Hemaprasanth, K.P., Sahoo, P.K., 2015. The immune response in rohu, *Labeo rohita* (Actinopterygii: Cyprinidae) to *Argulus siamensis* (Branchiura: Argulidae) infection: Kinetics of immune gene expression and innate immune response. Aquacult. Res. 46 (6), 1292–1308.

Kim, Y.E., Ahn, J.H., 2015. Positive role of promyelocytic leukemia protein in type I interferon response and its regulation by human cytomegalovirus. PLoS Pathog.11, e1004785.

Kumar, V., Roy, S., nu Barman, D., Kumar, A., Paul, L., Meetei, W.A., 2013. Immune evasion mechanism of parasites in fish. Aquaculture Europe. 38(2), 28-32

Langmead, B., Salzberg, S.L., 2012. Fast gapped-read alignment with Bowtie 2, Nat. Methods. 9, 357-359.

Liu, Y., Chen S.L., Meng, L., Zhang, Y.X., 2007. Cloning, characterization and expression analysis of a CXCL10-like chemokine from turbot (*Scophthalmus maximus*), Aquacult. 272, 199-207.

Livak, K.J., Schmittgen, T.D., 2001. Analysis of relative gene expression data using real time quantitative PCR and the 2 (-DD CT) method. Methods. 25, 402-8.

Lom, J., Lawler, A.R., 1973. An ultrastructural study on the mode of attachment in dinoflagellates invading gills of Cyprinodontidae. *Protistologica*, IX. (2), 293-309.

Mitter, K., Kotoulas, G., Magoulas, A., Mulero, V., Sepulcre, P., Figueras, A., Novoa, B., Sarropoulou, E., 2009. Evaluation of candidate reference genes for QPCR during ontogenesis and of immune relevant tissues of European seabass (*Dicentrarchus labrax*). Comp. Biochem. Physiol. B, Biochem. Mol. Biol. 153, 340–347.

Mitter, K., Kotoulas, G., Magoulas, A., Mulero, V., Sepulcre, P., Figueras, A., Novoa, B., Sarropoulou, E., 2009. Evaluation of candidate reference genes for QPCR during ontogenesis and of immune relevant tissues of European seabass (*Dicentrarchus labrax*). Comp. Biochem. Physiol. B Biochem. Mol. Biol.153, 340-347.

Mo, Z.Q., Li, Y.W., Wang, H.Q., Wang, J.L., Ni, L.Y., Yang, M., Lao, G.F., Luo, X.C., Li, A.X., Dan, X.M., 2016. Comparative transcriptional profile of the fish parasite *Cryptocaryon irritans*. Parasite Vector. 9, 630.

Mohd-Shaharuddin, N., Mohd-Adnan, A., Kua, B.C., Nathan, S., 2013. Expression profile of immune-related genes in *Lates calcarifer* infected by *Cryptocaryon irritans*. Fish Shellfish Immunol. 34, 762-769.

Montero, J., Coll, J., Sevilla, N., Cuesta, A., Bols, N.C., Tafalla, C., 2008. Interleukin 8 and CK-6 chemokines specifically attract rainbow trout (*Oncorhynchus mykiss*) RTS11 monocyte-macrophage cells and have variable effects on their immune functions. Dev. Comp. Immunol. 32, 1374-1384.

Nibbs, R.J., Graham, G.J., 2013. Immune regulation by atypical chemokine receptors. Nat Rev Immunol. 13, 815–29.

Nozzi, V., Strofaldi, S., Forner Piquer, I., Di Crescenzo, D., Olivotto, I., Carnevali, O., 2016. *Amyloodinum ocellatum* in *Dicentrarchus labrax*: study of infection in salt water and freshwater aquaponics. Fish Shellfish Immunol. 57, 179-185.

Oladiran, A., Beauparlant, D., Belosevic, M., 2011. The expression analysis of inflammatory and antimicrobial genes in the goldfish (*Carassius auratus* L.) infected with *Trypanosoma carassii*, Fish Shellfish Immunol. 31, 606–613.

Olsen, M.M., Kania, P.W., Heinecke, R.D., Skjoedt, K., Rasmussen, K.J., Buchmann, K., 2011. Cellular and humoral factors involved in the response of rainbow trout gills to *Ichthyophthirius multifiliis* infections: molecular and immunohistochemical studies. Fish Shellfish Immunol. 30(3), 859–69.

Page-McCaw, A., Ewald, A.J., Werb, Z., 2007. Matrix metalloproteinases and the regulation of tissue remodelling Nat. Rev. Mol. Cell Biol. 8, 221-233.

Piazzon, M.C., Mladineo, I., Naya-Català, F., Dirks, R.P., Jong-Raadsen, S., Vrbatovic, A., Hrabar, J., Pérez-Sánchez, J., Sitjà-Bobadilla, A., 2019. Acting locally - affecting globally: RNA sequencing of gilthead sea bream with a mild *Sparicotyle chrysophrii* infection reveals effects on apoptosis, immune and hypoxia related genes. BMC Genomics. 20, 200.

Podack, E.R., Young, J.D., Cohn, Z.A., 1985. Isolation and biochemical and functional characterization of perforin 1 from cytolytic T-cell granules. Proc Natl Acad Sci USA. 82(24), 8629–33.

Proudfoot, A.E., 2002. Chemokine receptors: multifaceted therapeutic targets. Nat Rev Immunol. 2, 106–15.

Raida, M.K., Buchmann, K., 2009. Innate immune response in rainbow trout (*Oncorhynchus mykiss*) against primary and secondary infections with *Yersinia ruckeri* O1. Dev. Comp. Immunol. 33 (1), 35-45.

Reyes-Becerril, M., Ascencio-Valle, F., Alamillo, E., Hirono, I., Kondo, H., Jirapongpairoj, W., & Angulo, C., 2015. Molecular cloning and comparative responses of Toll-like receptor 22 following ligands stimulation and parasitic infection in yellowtail (*Seriola lalandi*). Fish Shellfish Immunol. 46, 323–333.

Robledo, D., Ronza, P., Harrison, P.W., Losada, A.P., Bermúdez, R., Pardo, B.G., Redondo, M.J., Sitjà-Bobadilla, A., Quiroga, M.I., Martínez, P., 2014. RNA-seq analysis reveals significant transcriptome changes in turbot (*Scophthalmus maximus*) suffering severe enteromyxosis. BMC Genomics. 15, 1149.

826 Rodrigues, P.N., Vázquez-Dorado, S., Neves, J.V., Wilson J.M., 2006. Dual function of fish
827 hepcidin: response to experimental iron overload and bacterial infection in sea bass
828 (*Dicentrarchus labrax*). Dev Comp Immunol. 30, 1156-1167.

829 Ronza, P., Robledo, D., Bermúdez, R., Losada, A.P., Pardo, B.G., Sitjà-Bobadilla, A., Quiroga,
830 M.I., Martínez, P., 2016. RNA-Seq analysis of early enteromyxosis in turbot (*Scophthalmus*
831 *maximus*): New insights into parasite invasion and immune evasion strategies. Int. J.
832 Parasitol. 46, 507–517.

833 Saraiva, A., Jerónimo, D., Cruz, C., 2011. *Amyloodinium ocellatum* (Chromalveolata:
834 Dinoflagellata) in farmed turbot. Aquacult. 320, 34–36.

835 Secombes. C.J., Wang, T., Hong, S., Peddie, S., Crampe, M., Laing, K.J., Cunningham, C., Zou,
836 J., 2001. Cytokines and innate immunity of fish. Dev Comp Immunol. 25, 713–23.

837 Sigh, J., Lindenstrom, T., Buchmann, K., 2004a. Expression of pro-inflammatory cytokines in
838 rainbow trout (*Oncorhynchus mykiss*) during an infection with *Ichthyophthirius multifiliis*.
839 Fish Shellfish Immunol. 17 (1), 75–86.

840 Sigh, J., Lindenstrom, T., Buchmann, K., 2004b. The parasitic ciliate *Ichthyophthirius multifiliis*
841 induces expression of immune relevant genes in rainbow trout, *Oncorhynchus mykiss*
842 (Walbaum). J fish dis. 27(7), 409–17.

843 Sitjà-Bobadilla, A., 2008. Living off a fish: A trade-off between parasites and the immune system.
844 Fish Shellfish Immunol. 25, 358-372.

845 Smith, S.A., Levy, M.G., Noga, E.J., 1994. Detection of anti-Amyloodinium ocellatum anti-body
846 from cultured hybrid striped bass (*Morone saxatilis* x *M. chrysops*) during an epizootic of
847 amyloodiniosis. J. Aquat. Anim.Health. 6, 79-81.

848 Smythies, L.E., Maheshwari, A., Clements, R., Eckhoff, D., Novak, L., Vu, H.L., Mosteller-
849 Barnum, L.M., Sellers, M., Smith, P.D., 2006. Mucosal IL-8 and TGF-beta recruit blood
850 monocytes: evidence for cross talk between the lamina propria stroma and myeloid cells, J.
851 Leukoc. Biol. 80, 492-499.

852 Soares, F., Quental-Ferreira, H., Moreira, M., Cunha, E., Ribeiro, L., Pousão-Ferreira, P., 2012.
853 First report of *Amyloodinium ocellatum* in farmed meagre (*Argyrosomus regius*). Bull. Eur.
854 Ass. Fish Pathol. 32, 30-33.

855 Stone, M.J., Hayward, J.A., Huang, C., Huma, Z.E., Sanchez, J., 2017. Mechanisms of regulation
856 of the chemokine-receptor network. Int. J. Mol. Sci. 18, 342.

Sudhagar, A., Kumar, G., El-Matbouli, M., 2018. Transcriptome Analysis Based on RNA-Seq in Understanding Pathogenic Mechanisms of Diseases and the Immune System of Fish: A Comprehensive Review. Int. J. Mol. Sci. 19, 245.

Suresh, P., Wanchu, A., 2006. Chemokines and chemokine receptors in HIV infection: role in pathogenesis and therapeutics. J Postgrad Med. 52, 210–7.

Syahputra, K., Kania, P.W., Al-Jubury, A., Jafaar, R.M., Dirks, R.P., Buchmann, K., 2019. Transcriptomic analysis of immunity in rainbow trout (*Oncorhyncus mykiss*) gills infected by *Ichthyophthirius multifiliis*. Fish Shellfish Immunol. 86, 486-496.

Taylor, E.B., Moulana, M., Stuge, T.B., Quiniou, S.M.A., Bengten, E., Wilson, M. A., 2016. Leukocyte Immune-Type Receptor Subset Is a Marker of Antiviral Cytotoxic Cells in Channel Catfish, *Ictalurus punctatus*. J Immunol.196(6), 2677.

Tian, F., Tong, C., Feng, C., Kunyuan Wanghe, K., Zhao, K., 2017. Transcriptomic profiling of Tibetan highland fish (*Gymnocypris przewalskii*) in response to the infection of parasite ciliate *Ichthyophthirius multifiliis*. Fish Shellfish Immunol. 70, 524-535.

Toda, H., Araki, K., Moritomo, T., Nakanishi, T., 2011. Perforin-dependent cytotoxic mechanism in killing by CD8 positive T cells in ginbuna crucian carp, *Carassius auratus* langsdorfii. Dev Comp Immunol. 35(1), 88–93.

Van den Steen, P.E., Dubois, B., Nelissen, I., Rudd, P.M., Dwek, R.A., Opdenakker, G., 2002. Biochemistry and molecular biology of gelatinase B or matrix metalloproteinase-9 (MMP-9). Crit. Rev. Biochem. Mol. Biol. 37, 375-536.

Varela, M., Forn-Cuní, G., Dios, S., Figueras, A., Novoa, B., 2016. Proinflammatory Caspase a activation and an antiviral state are induced by a zebrafish perforin after possible cellular and functional diversification from a myeloid ancestor. J Innate Immun. 8(1), 43–56.

Volkman, H.E., Pozos, T.C., Zheng, J., Davis, J.M., Rawls, J.F., Ramakrishnan. L., 2010. Tuberculous Granuloma Induction via Interaction of a Bacterial Secreted Protein with Host Epithelium. Science. 327, 466-469.

Wang, P., Wang, J., Su, Y.Q., Mao, Y., Zhang, J.S., Wu, C.W., Ke, Q.Z., Han, K.H., Zheng, W.Q., Xu, N.D., 2016. Transcriptome analysis of the *Larimichthys crocea* liver in response to *Cryptocaryon irritans*. Fish Shellfish Immunol. 48, 1–11.

Wood, P., 2011. Understanding Immunology. 3rd ed: Pearson Education Limited, England; 2011.

887 Xu, Z., Parra, D., Gomez, D., Salinas, I., Zhang, Y.A., von Gersdorff Jorgensen, L., Heinecke,
888 R.D., Buchmann, K., LaPatra, S., Sunyer, J.O., 2013. Teleost skin, an ancient mucosal
889 surface that elicits gut-like immune responses. Proc. Natl. Acad. Sci. U.S.A. 110, 13097-
890 13102.

891 Yin, F., Gao, Q., Tang, B., Sun, P., Han, K., Huang, W., 2016. Transcriptome and analysis on the
892 complement and coagulation cascades pathway of large yellow croaker (*Larimichthys*
893 *crocea*) to ciliate ectoparasite *Cryptocaryon irritans* infection. Fish Shellfish Immunol. 50,
894 127–141.

895 Yin, F., Sun, P., Wang, J., Gao, Q., 2016. Transcriptome analysis of dormant tomonts of the marine
896 fish ectoparasitic ciliate *Cryptocaryon irritans* under low temperature. Parasites Vectors. 9,
897 280.

898 Young, N.D., Cooper, G.A., Nowak, B.F., Koop, B.F., Morrison, R.N., 2008. Coordinated down-
899 regulation of the antigen processing machinery in the gills of amoebic gill disease-affected
900 Atlantic salmon (*Salmo salar* L.). Mol. Immunol. 45, 2581–2597.

901 Zhang, YA., Li, J., Parra, D., Bjork, S., Xu, S., LaPatra, S.E., Bartholomew, J., Sunyer J.O., 2010.
902 IgT, a primitive immunoglobulin class specialized in mucosal immunity. Nat. Immunol.
903 11,827-835.

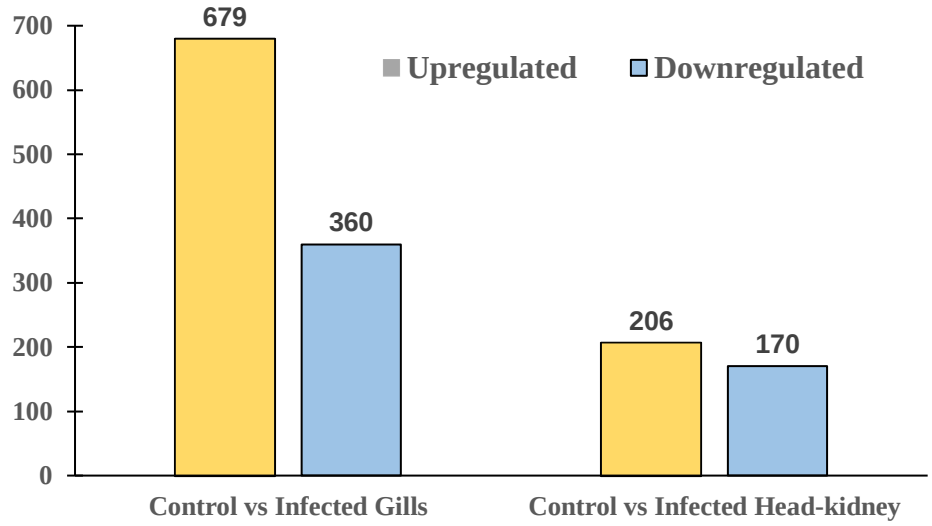

Figure 1 - Upregulation and down regulation of differentially expressed genes in gills and head kidney after challenge with *A. ocellatum* in *D. labrax*.

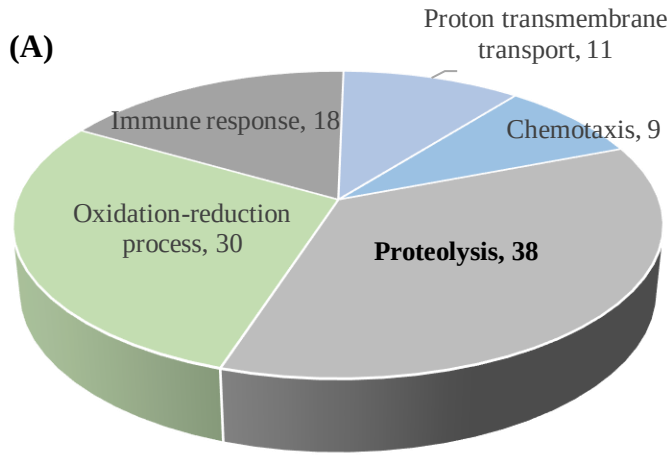
(A)
Proton transmembrane transport, 11
Chemotaxis, 9
Immune response, 18
Oxidation-reduction process, 30
Proteolysis, 38

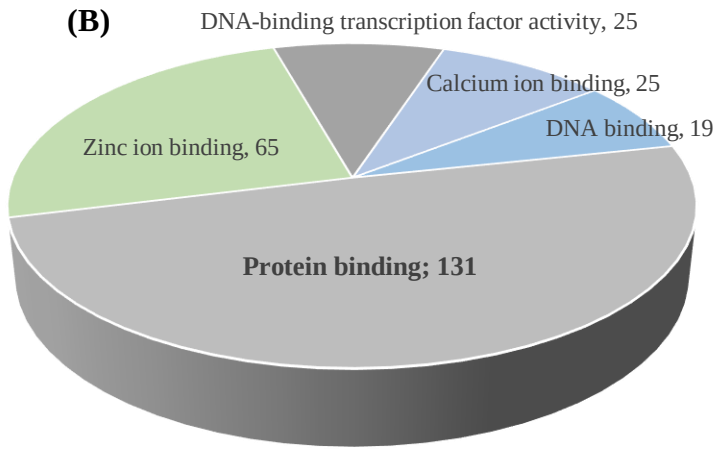
(B)
DNA-binding transcription factor activity, 25
Calcium ion binding, 25
DNA binding, 19
Zinc ion binding, 65
Protein binding; 131

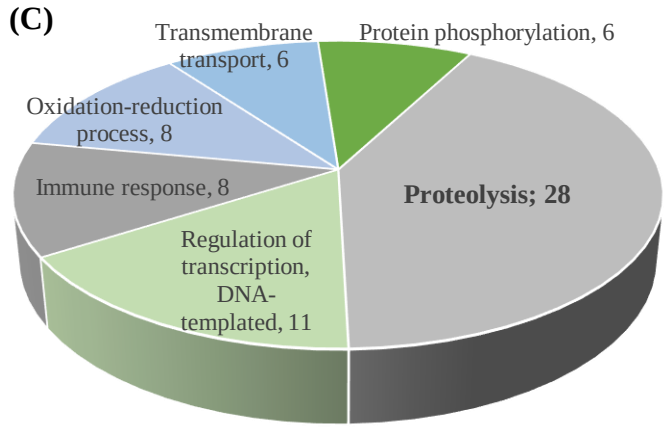
(C)
Transmembrane transport, 6
Protein phosphorylation, 6
Oxidation-reduction process, 8
Immune response, 8
Regulation of transcription, DNA-templated, 11
Proteolysis; 28

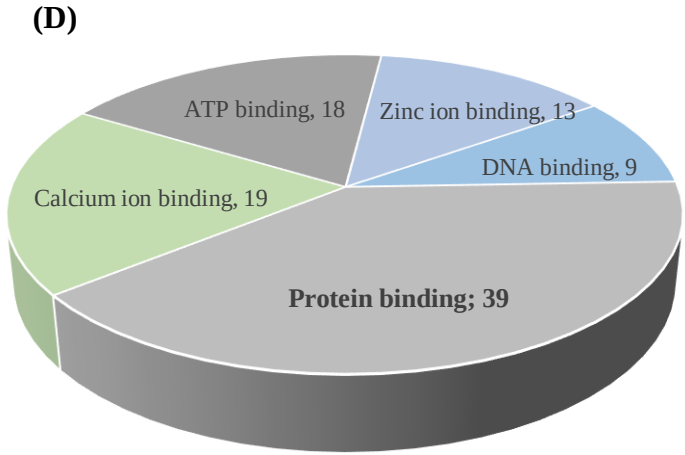
(D)
ATP binding, 18
Zinc ion binding, 13
DNA binding, 9
Calcium ion binding, 19
Protein binding; 39

Figure 2. Gene ontology (GO) enrichment analysis of differentially expressed genes in gills (a & b) and head kidney (c & d). The results of GO enrichment analysis of differentially expressed genes were classified into two categories: biological process (a and c), and molecular function (b & d). The functional classification of GO with the corresponding number of genes.

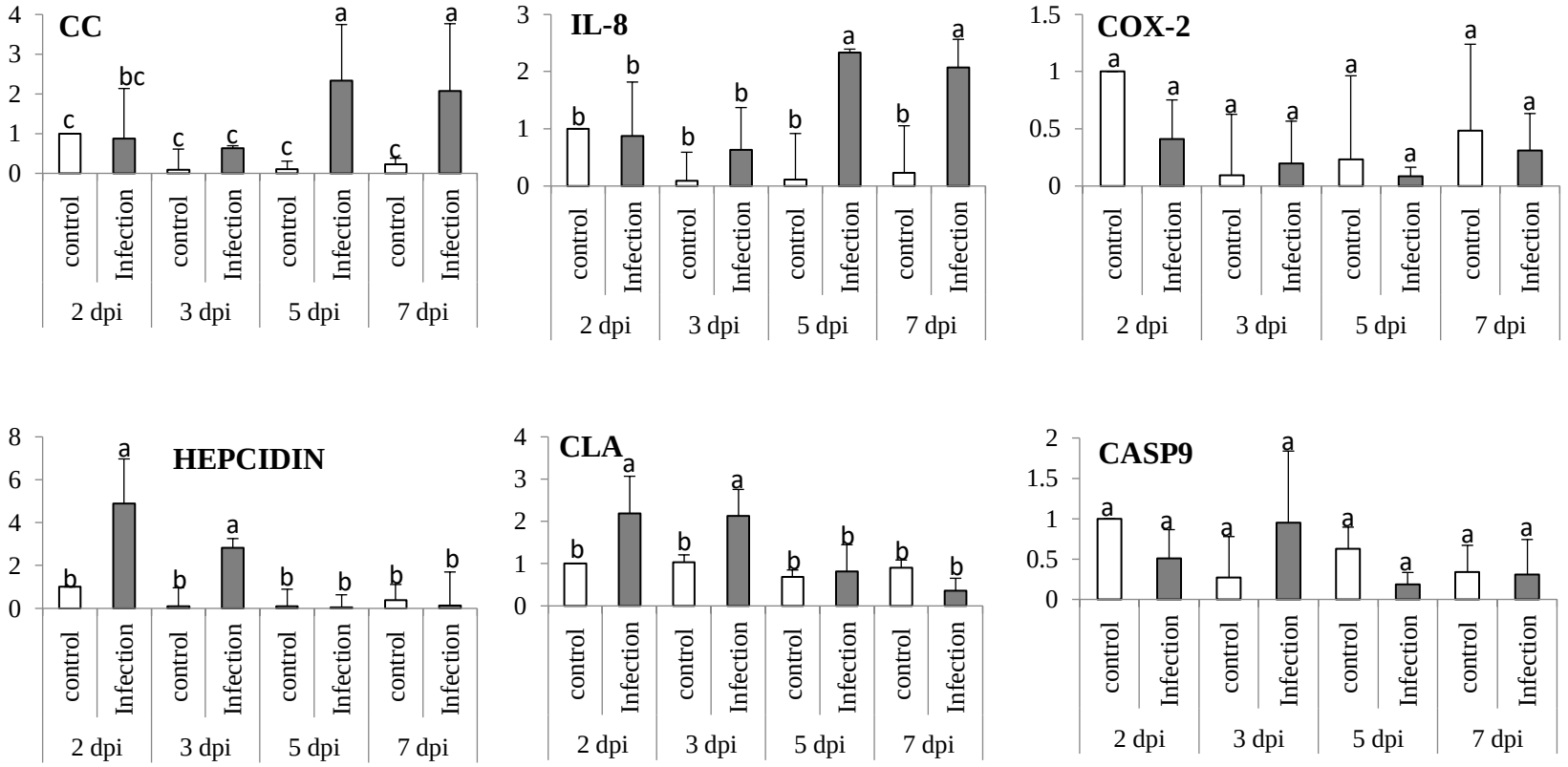

Figure 3- Relative mRNA expression of innate, immune-related genes chemokine CC1, interleukin-8, cyclooxygenase-2, hepcidin, c-type lectin A and Caspase-9 at 2, 3, 5, 7 days post infection **in gills of ESB** infested with AO as measured by quantitative real-time PCR. Data are presented as mean ± SD and multiple reference genes were used to normalize with the target gene (n=3). Different alphabetical letters indicate the significant difference with $p<0.05$.

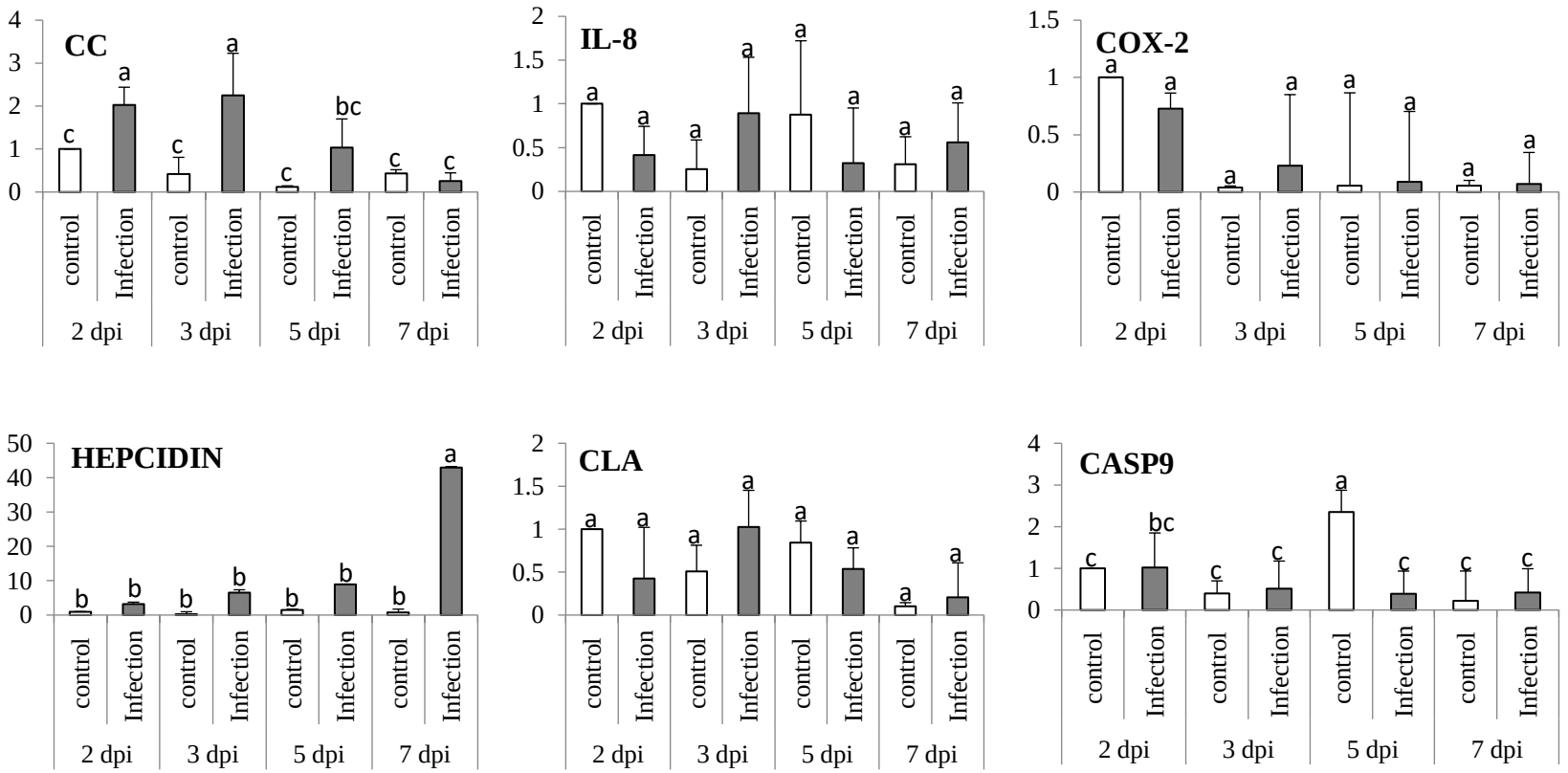

Figure 4- Relative mRNA expression of innate, immune related genes chemokine CC1, interleukin-8, cyclooxygenase-2, hepcidin, c-type lectin A and Caspase-9 at 2, 3, 5, 7 days post infection **in head kidney** of ESB infested with AO as measured by quantitative real-time PCR. Data are presented as mean ± SD and multiple reference genes were used to normalize with the target gene (n=3). Different alphabetical letters indicate the significant difference with $p<0.05$.

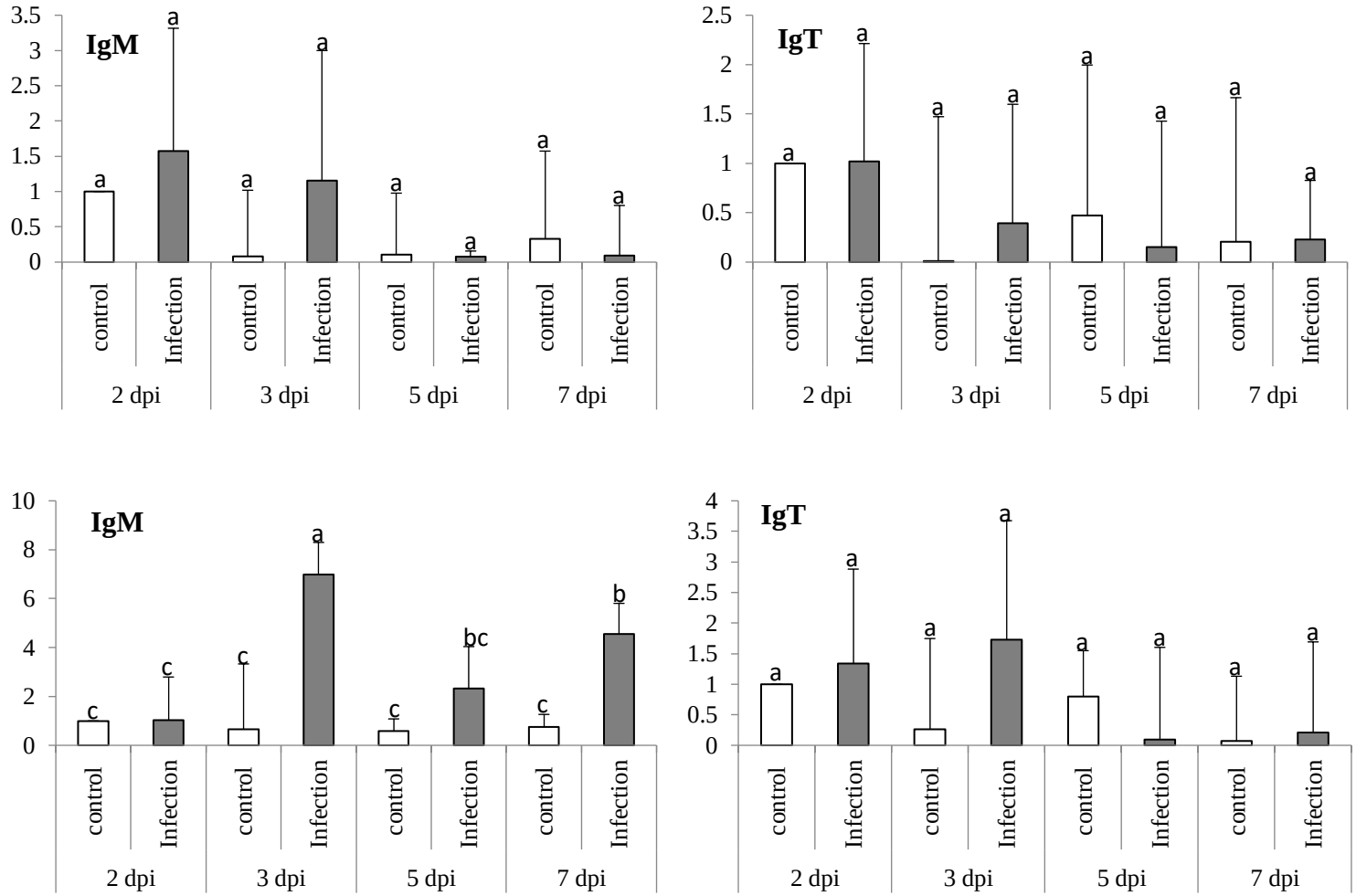

Figure 5- Relative mRNA expression of immunoglobulin M and immunoglobulin T at 2, 3, 5, 7 days post infested **in gills (A and B) head kidney (C and D) of ESB** infected with AO as measured by quantitative real-time PCR. Data are presented as mean ± SD and multiple reference genes were used to normalize with the target gene (n=3). Different alphabetical letters indicate the significant difference with $p<0.05$.

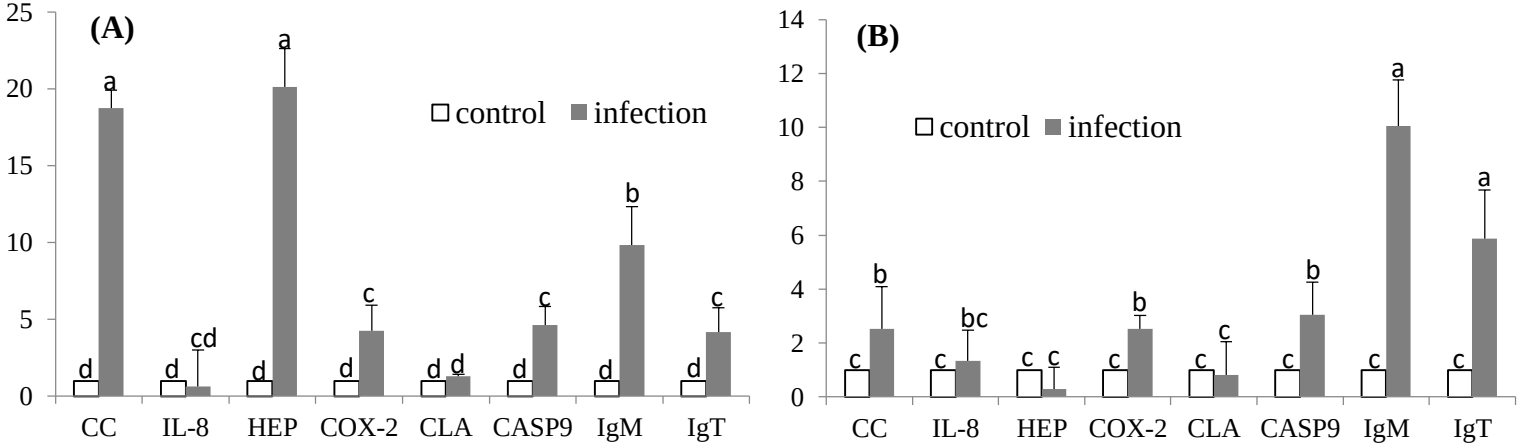

Figure 6- Relative mRNA expression of immune genes at 23 days post infection **in gills (A)** and **head kidney (B)** of ESB infested with AO as measured by quantitative real-time PCR. Data are presented as mean ± SD and multiple reference genes were used to normalize with the target gene (n=3). Different alphabetical letters indicate the significant difference with $p<0.05$.

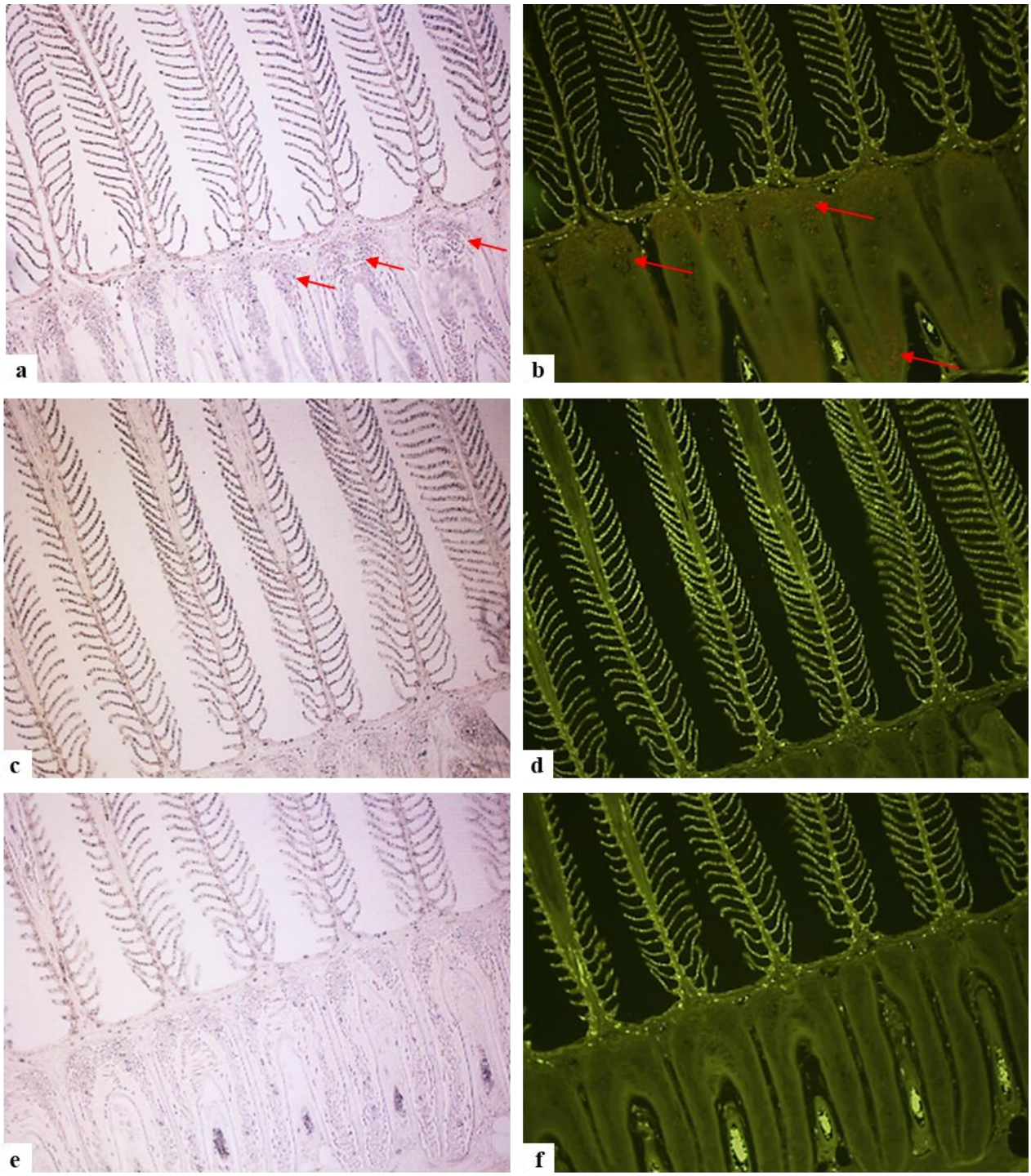

Figure 7. ESB gill tissue from uninfested control fish. a) and b) Leukocytes expressing Chemokine CC1 in the GIALT (Gill Associated Lymphoid Tissue) (arrows). c) and d) sections incubated with Chemokine CC1 sense probe. e) and f) Negative control (no riboprobes). Images captured in brightfield are on the left, images captured using fluorescence microscopy are on the right. All at 10X magnification.

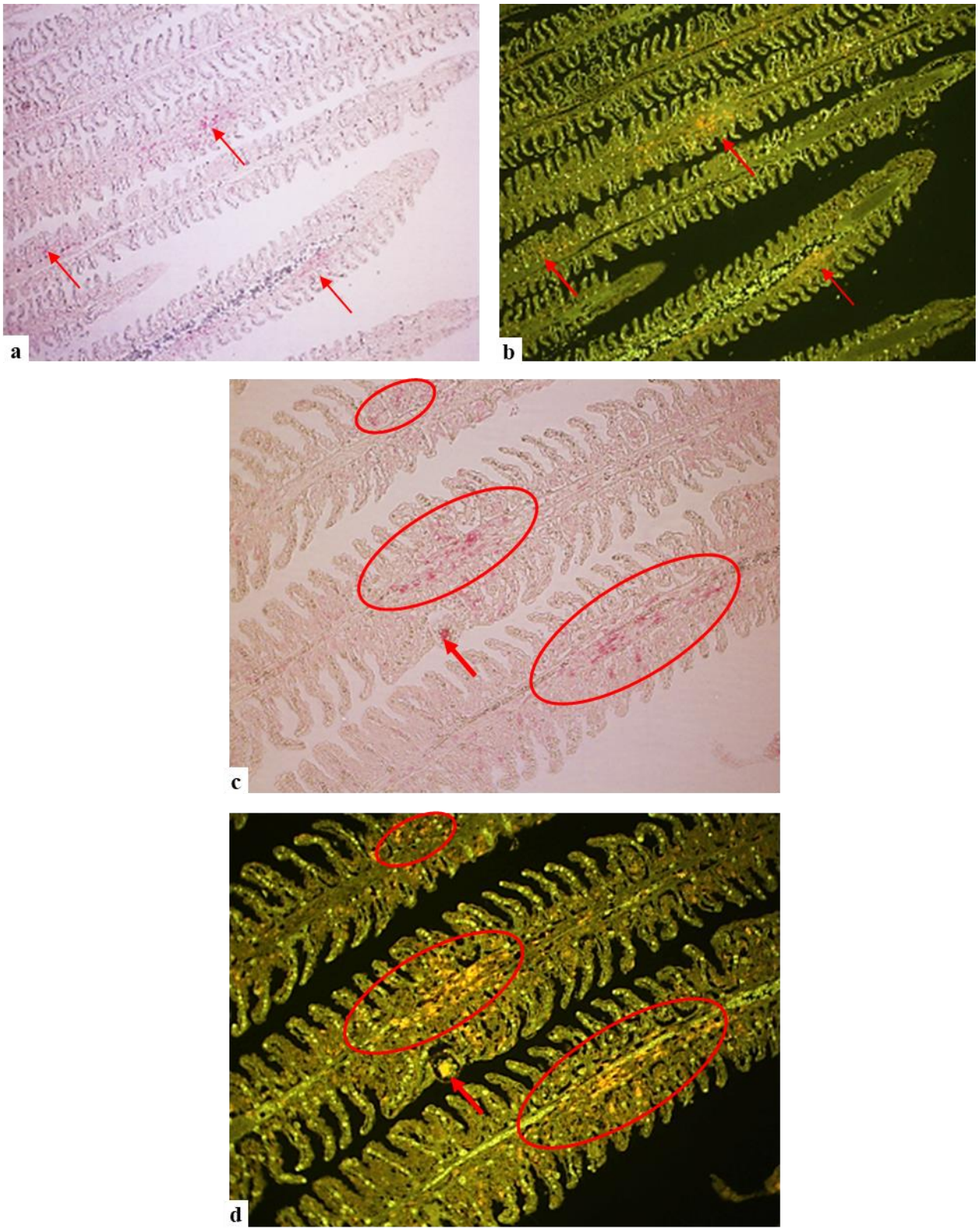

Figure 8. ESB gill tissue infested by *A. ocellatum*. a) to d) CC1 positive leukocytes in the hyperplastic regions of the secondary lamellae and in the vessel wall (diapedesis) of the central

venous sinus of the primary lamellae. c) and d) A positive signal for CC1 in the hyperplastic areas of secondary lamellae and within cytoplasm of *A. ocellatum* trophonts (arrows). a) and b) 10X magnification; c) and d) 20X magnification. Images 8a and 8c were captured in brightfield, figures 8b and 8d using fluorescence.

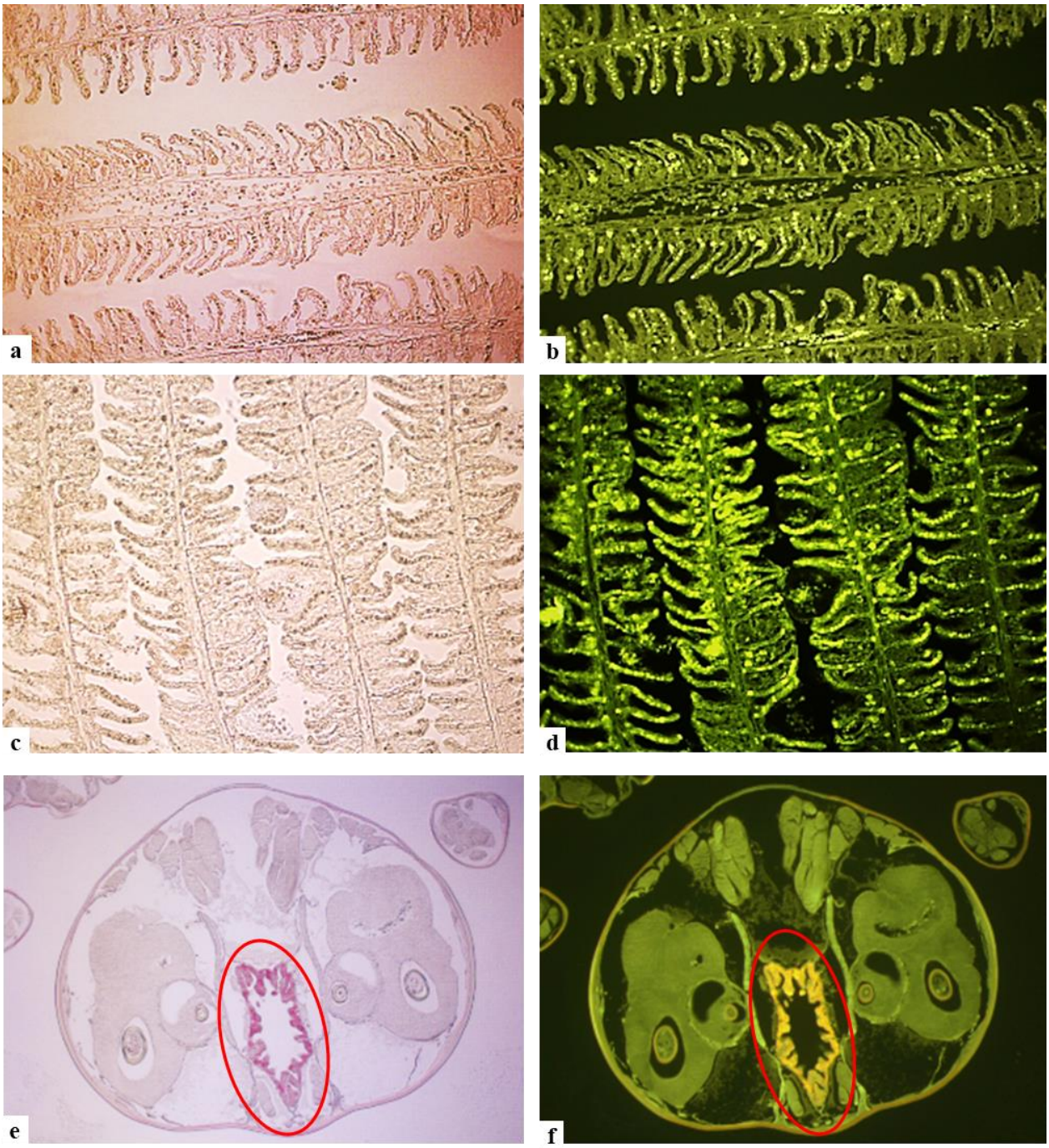

Figure 9. ESB gill tissue infested by *A. ocellatum*. a) and b) Chemokine CC1 sense probe, 10X magnification. c) and d) Negative control (no riboprobes), 20X magnification. e) and f) Reference positive control represented by sea louse (*L. salmonis*) intestine labelled with Trypsin antisense probe, 10X magnification. Images on the left captured with brightfield and on the right using fluorescence.

Table 1a. Functional group, name and sequence of genes of interest and three reference genes. Primers were either designed using sequences from GenBank (see accession number) or taken from literature (see reference).

	Functional group	*Name*	Forward Sequence	*Name*	Reverse Sequence	GenBank Accession number
1	***Innate Immunity***	*cc1-F*	tgggttcgccgcaaggttgtt	*cc1-R*	agacagtagacgaggggaccacaga	AM490065.1
2		*il8-F*	gtctgagaagcctgggagtg	*il8-R*	gcaatgggagttagcaggaa	AM490063.1
3		*hep-F*	aagagctggaggagccaatgagca	*hep-R*	gactgctgtgacgcttgtgtctgt	DQ131605.1
4		*cox2-F*	agcacttcacccaccagttc	*cox2-R*	aagcttgccatccttgaaga	Cordero *et al*., 2016
5	***Adaptive immunity***	*Ighm-F*	aggacaggactgctgctgtt	*ighm-R*	acaacagcagacagcaggtg	AM493677
6		*Ight-F*	cggacttcattcagtaccctg	*Ight-R*	caactgtacacatcagggcc	KM410929.1
7	***Complement system***	*cla-F*	gatggcagcaagctccggtattca	*cla-R*	tctgacctatgaccccagccaaca	EU660935.1
8		*casp9-F*	ggcaggactcgacgagatag	*casp9-R*	ctcgctctgaggagcaaact	DQ345776.1
9	***Reference***	*actb-F*	tgaaccccaaagccaacagggaga	*actb-R*	gtacgaccagaggcatacagggaca	AJ537421.1
10		*l13a-F*	tctggaggactgtcaggggcatgc	*l13a-R*	agacgcacaatcttgagagcag	Mitter *et al*., 2009
11		*hsp90-F*	gctgacaagaacgacaaggctgtga	*hsp90-R*	agatgcggttggagtgggtctgt	AY395632.1

Table 1b. Primers plus T7 region used for designing the riboprobes for mRNA FISH.

Probes	Oligo name	Sequence (5' → 3')
Chemokine CC1 sense probe	Chemo2_T7_FW	taatacgactcactatagggtctctggagaggaacggaga
	Chemo2RV	ggtgttttcattggccggag
Chemokine CC1 antisense probe	Chemo2FW	tctctggagaggaacggaga
	Chemo2_T7_RV	taatacgactcactatagggggtgttttcattggccggag

Table 2. Differentially expressed genes (DEGs) regulated after AO infestation in gills of ESB.

Annotation	Gene abbreviation	Gene name	Fold change	Up / downregulated
Immune response	*ccl21*	c-c motif chemokine 21-like	581,78	↑
	cc1	cc chemokine 1	46,32	↑
	il12a	interleukin-12 subunit alpha-like	39,66	↑
	il10	interleukin 10	5,52	↑
	gcsf	granulocyte colony-stimulating factor-like	5,18	↑
	tnfsf12	tumor necrosis factor ligand superfamily member 12-like	-14,44	↓
	sbspon	somatomedin-b and thrombospondin type-1	-1,70	↓
	tnfs13b	tumor necrosis factor ligand superfamily member 13b	-1,50	↓
	tnf-α	tumor necrosis factor alpha	-1,40	↓
	tnfs10	tumor necrosis factor ligand superfamily member 10-like	-1,31	↓
Proteolysis	*mmp*	matrix metalloproteinase	113,40	↑
	spe	elastase-like serine protease	41,32	↑
	pcsk6	proprotein convertase subtilisin kexin type 6	39,86	↑
	casp3	caspase 3b	38,12	↑
	cela1	pancreatic elastase	35,86	↑
	mts16	metalloproteinase with thrombospondin motifs 16	-341,9	↓
	f11	coagulation factor xi-like	-102,69	↓
	cpa6	carboxypeptidase a6	-25,94	↓
	klk8	kallikrein-8 precursor	-13,78	↓
	capn15	calpain-15	-13,69	↓
Protein binding	*ankrd1*	ankyrin repeat domain-containing protein 1	616,50	↑
	ctnnd2	catenin delta-2	139,42	↑
	ifi17	interferon-induced 17 kda protein precursor	101,52	↑
	il28b	interleukin-27 subunit beta-like	93,41	↑
	nlrc3	protein nlrc3-like	88,88	↑
	ankdd1b	ankyrin repeat and death domain-containing protein 1b	-8,20	↓
	ptprj	receptor-type tyrosine-protein phosphatase eta-like	-7,79	↓
	muc5ac	mucin-5ac- partial	-6,75	↓
	f11	coagulation factor xi-like	-6,68	↓
	c3	complement component c3	-5,26	↓

Table 3. Differentially expressed genes (DEGs) regulated after AO infestation in head kidney of ESB.

Annotation	Gene abbreviation	Gene name	Fold change	Up / downregulated
Immune response	*cc1*	cc chemokine 1	22,97	↑
	il10	interleukin 10 precursor	22,40	↑
	cxc10	c-x-c motif chemokine 10 precursor	13,66	↑
	cxc19	c-c motif chemokine 19 precursor	11,45	↑
	cc21	c-c motif chemokine 21-like	7,30	↑
	sbspon	somatomedin-b and thrombospondin type-1	-6,19	↓
	tnfsf10	tumor necrosis factor ligand superfamily member 10-like	-4,08	↓
	tnf-α	tumor necrosis factor alpha	-2,50	↓
	c9	complement component c9	-1,47	↓
	eda	ectodysplasin splice variant-8 exons	-1,17	↓
Proteolysis	*ddn1*	duodenase-1 precursor	50,99	↑
	bmp1	bone morphogenetic protein 1	20,57	↑
	mmp	matrix metalloproteinase	19,63	↑
	mcpt1	mast cell protease 1a-like	18,34	↑
	gzma	granzyme a-like	14,22	↑
	cpb	carboxypeptidase b	-272,84	↓
	ctrb	chymotrypsin b-like	-252,15	↓
	prss1	trypsin-1 precursor	-221,94	↓
	ctr2	chymotrypsinogen 2	-185,22	↓
	trp	trypsinogen 2	-174,21	↓
Protein binding	*trim39*	e3 ubiquitin-protein ligase trim39-like	129,68	↑
	nlrc3	protein nlrc3-like	79,16	↑
	ifi17	interferon-induced 17 kda protein precursor	77,45	↑
	setd8	n-lysine methyltransferase setd8-like	31,95	↑
	sdk2	protein sidekick-2-like	-189,87	↓
	mybpc1	myosin-binding protein slow-type	-124,58	↓
	mxra5	matrix-remodeling-associated protein 5	-112,65	↓
	cntn4	contactin-4-like	-98,96	↓
	klhl34	kelch-like protein 34	-90,95	↓

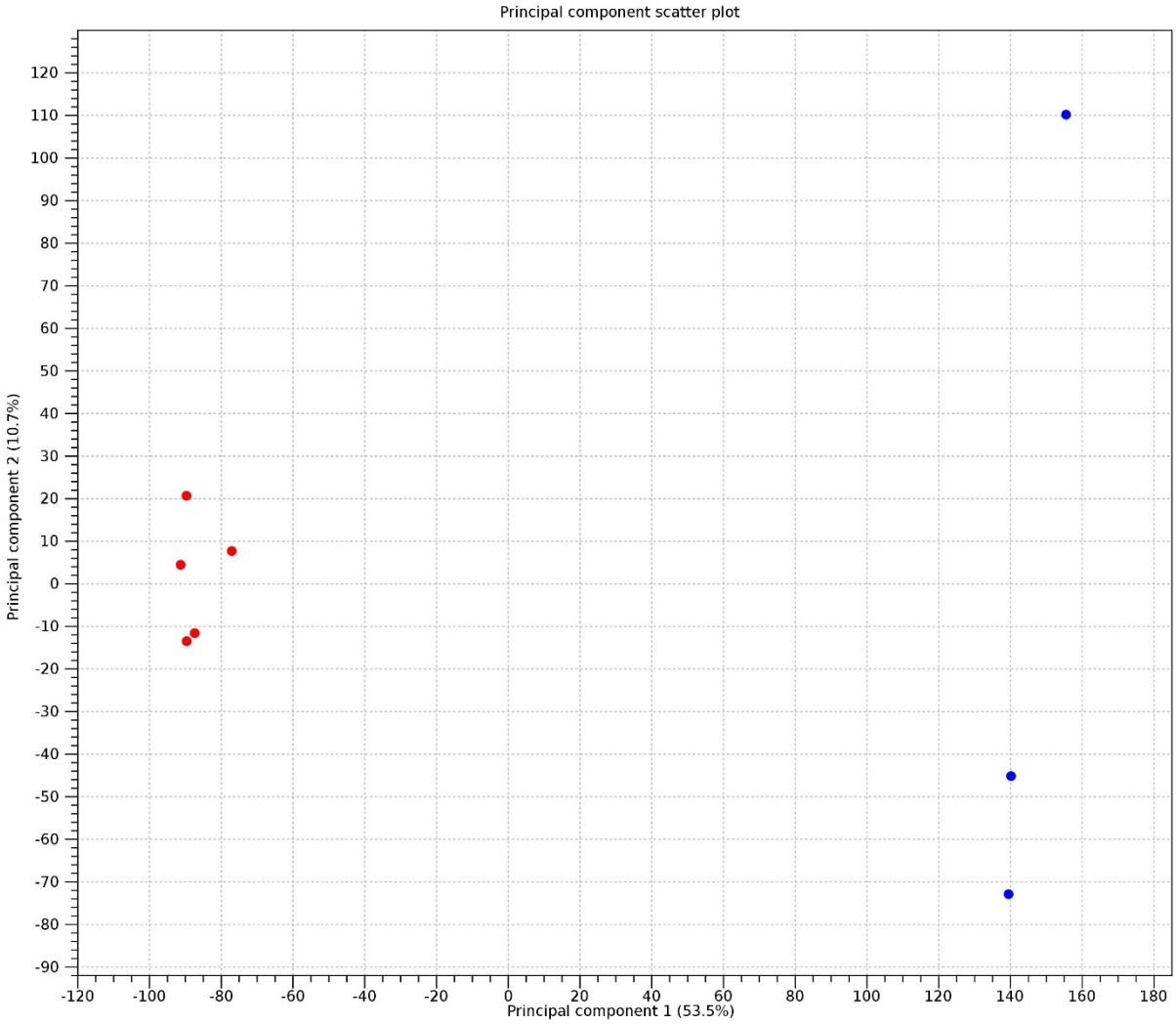

Supplementary Figure 1- Principal component analysis (PCA) of the normalized RNA-seq data transcripts per million (TPM) of *D. labrax* gills in response to infestation with *A. ocellatum*. Red dot represents infested gills and blue dot indicates non-infested gills.

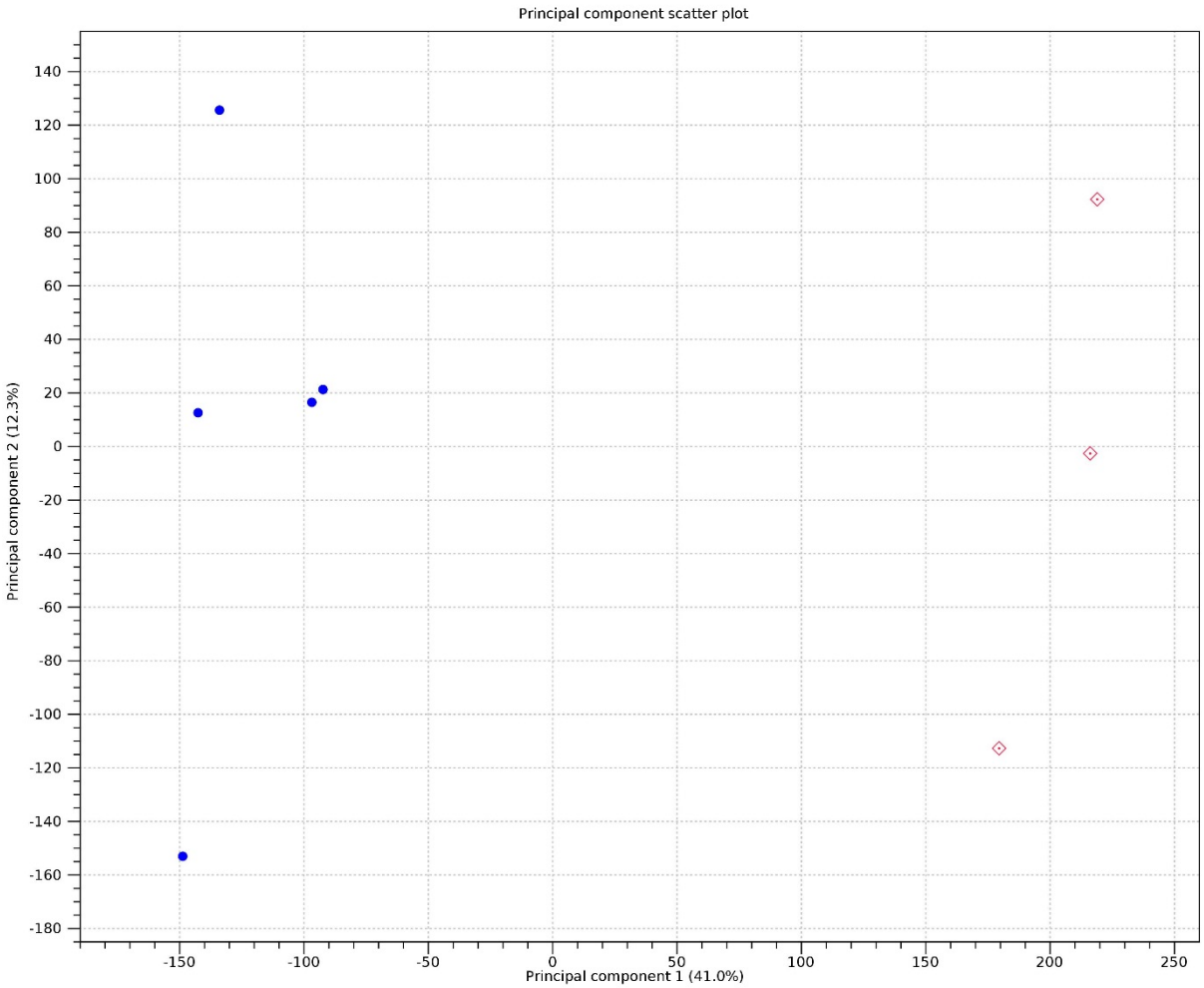

Supplementary Figure 2- Principal component analysis (PCA) of the normalized RNA-seq data transcripts per million (TPM) of *D. labrax* head kidney in response to infestation with *A. ocellatum*. Blue dot represents infested head kidney and red dot indicates non-infested head kidney.

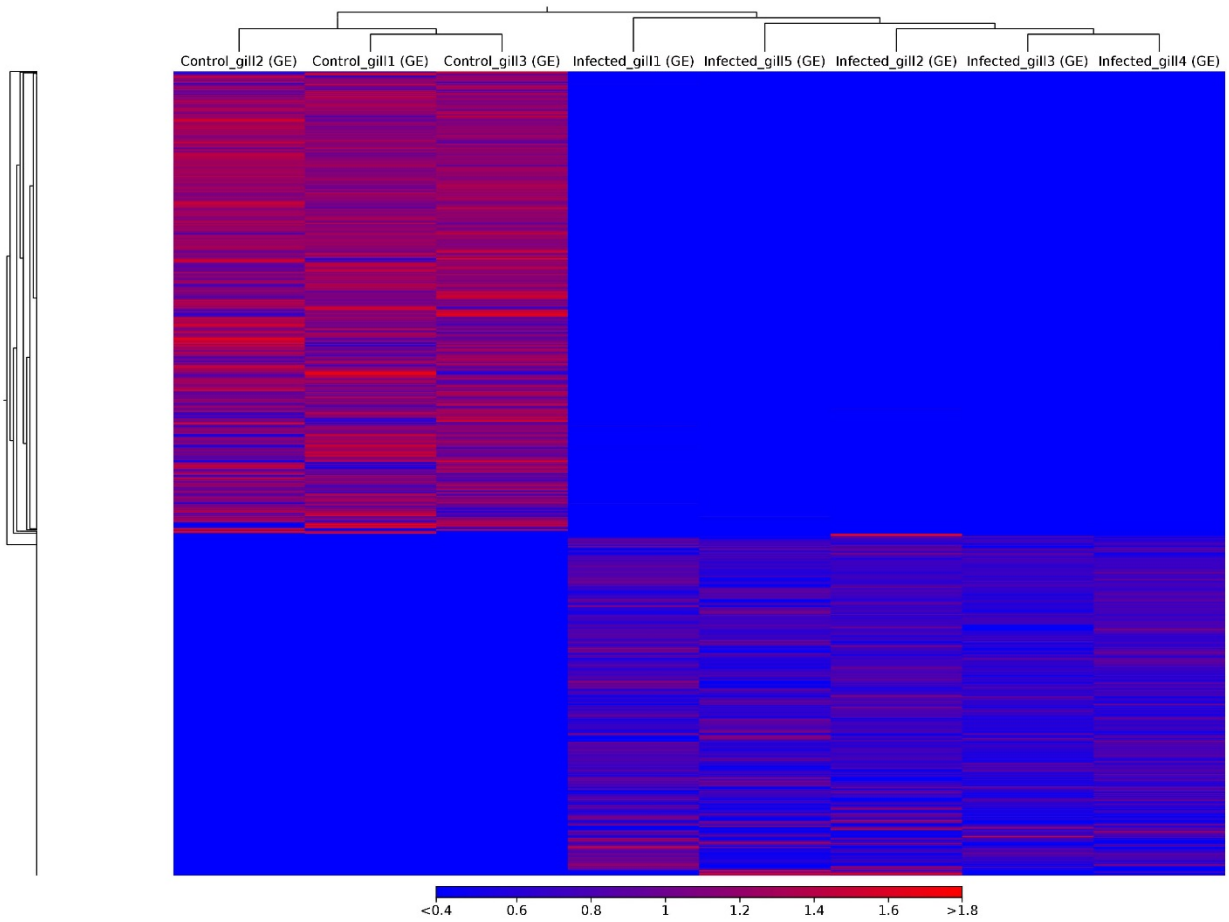

Supplementary Figure 3- A heat map based on gene expression levels of 1039 DEGs in gills of *D. labrax* infested with *A. ocellatum*. Hierarchical clustering heatmaps based on the DESeq-normalized gene expression levels. The genes with similar expression patterns are clustered together. The up-regulated genes are in red and the down-regulated genes are in blue.

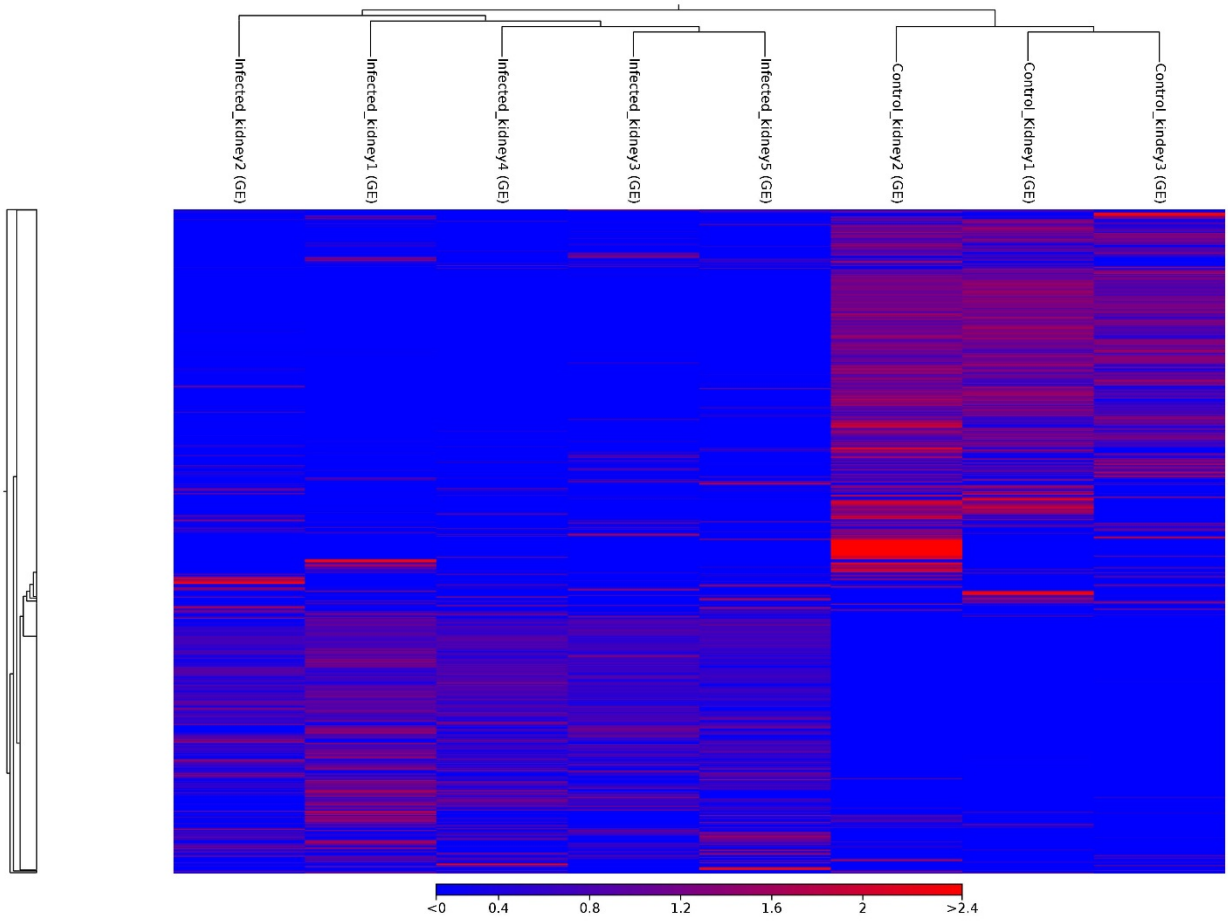

Supplementary Figure 4 - A heat map based on gene expression levels of 376 DEGs in head kidney of D. labrax infested with *A. ocellatum*. Hierarchical clustering heat maps based on the DESeq-normalized gene expression levels. The genes with similar expression patterns are clustered together. The up-regulated genes are in red and the down-regulated genes are in blue.

Supplementary Table 1. Read count statistics

Sample name	Read count	GC content %	Paired, mapped pairs %	Paired, broken pairs %	Paired, not mapped %
Control_gill1	23,160,288	54	65.20	17.24	17.57
Control_gill2	22,780,654	52	72.37	9.01	18.62
Control_gill3	19,241,532	54	62.81	18.24	18.95
Control_Kidney1	21,220,732	52	55.56	26.64	17.81
Control_Kidney2	21,777,880	54	62.76	19.77	17.47
Control_Kidney3	23,005,570	52	64.53	18.76	16.71
Infested_gill1	19,071,872	50	60.16	22.68	17.16
Infested_gill2	28,364,912	52	61.55	20.70	17.76
Infested_gill3	26,269,084	50	67.99	15.56	16.44
Infested_gill4	24,975,596	52	70.73	13.86	15.42
Infested_gill5	27,012,904	52	58.24	23.23	18.53
Infested_Kidney1	23,440,752	50	60.88	23.14	15.99
Infested_Kidney2	20,271,424	52	58.06	23.41	18.53
Infested_Kidney3	25,841,066	52	62.37	22.07	15.55
Infested_Kidney4	20,184,678	52	60.59	23.45	15.96
Infested_Kidney5	26,524,480	52	62.86	21.88	15.25

Supplementary Table 2. Fragment count statistics

Sample name	Mapped to genes %	Mapped to intergenic %
Control_gill1	90.31	9.69
Control_gill2	87.66	12.34
Control_gill3	90.36	9.64
Control_Kidney1	93.92	6.08
Control_Kidney2	93.77	6.23
Control_Kindey3	93.83	6.17
Infested_gill1	91.65	8.35
Infested_gill2	92.36	7.64
Infested_gill3	92.14	7.86
Infested_gill4	92.11	7.89
Infested_gill5	92.02	7.98
Infested_Kidney1	94.63	5.37
Infested_Kidney2	94.85	5.15
Infested_Kidney3	94.88	5.12
Infested_Kidney4	95.37	4.63
Infested_Kidney5	95.27	4.73

Supplementary Table 3 - List of top 20 Upregulated and Downregulated genes in gills of *D. labrax* infested with *A. ocellatum* representing gene symbol, protein product, gene ontology class and fold change.

UPREGULATED				
Ranking	**Gene symbol**	**Protein product**	**GO Class (Direct)**	**Fold change**
1	*prf1*	perforin-1-like	immune system	1,806.91
2	*gimap4*	gtpase imap family member 4-like	cytosol	800.18
3	*rtp3*	receptor-transporting protein 3	protein binding	675.40
4	*ankrd1*	ankyrin repeat domain-containing protein 1	ankyrin repeat binding	616.50
5	*gig2*	gig2-like protein	cytoplasm	541.34
6	*ifit5*	interferon-induced protein with tetratricopeptide repeats 1-like	protein binding	439.90
7	*aloxe3*	epidermis-type lipoxygenase 3-like	epidermis development	437.59
8	*samd9*	sterile alpha motif domain-containing protein 9	protein binding	436.05
9	*gadl1*	glutamate decarboxylase-like protein 1	protein binding	252.53
10	*gcnt1*	beta- -galactosyl-o-glycosyl-glycoprotein beta- -n-acetylglucosaminyltransferase-like	oxidation-reduction process	251.50
11	*asrgl1*	isoaspartyl peptidase l-asparaginase	beta-aspartyl-peptidase activity	241.82
12	*noxo1*	nadph oxidase organizer 1-like	NADPH oxidase complex	172.73
13	*tuba1a*	tubulin alpha-1a chain	structural constituent of cytoskeleton	160.62
14	*hsp70*	heat shock protein 70	regulation of protein ubiquitination	134.98
15	*cc1*	cc chemokine 1	chemokine activity	117.50
16	*nf-x-like*	melanophilin-like isoform x1	integral component of membrane	115.70
17	*cxcr1*	c-x-c chemokine receptor type 1-like	chemokine binding	115.07
18	*arg1*	arginase-1	cytoplasm	109.71
19	*viperin*	Virus inhibitory protein	suppression by virus of host transcription	109.08
20	*cnfn*	cornifelin homolog b-like	cytoplasm	79.15
DOWNREGULATED				
Ranking	**Gene symbol**	**Protein product**	**GO Class (Direct)**	**Fold change**
1	*tgm1*	Protein-glutamine gamma-glutamyltransferase 5 isoform 1	eukaryotic initiation factor 4E binding	-2,151.91
2	*casp1*	caspase 1 isoform 2	protein binding	-169.66
3	*gast*	gastrin cholecystokinin-like peptide-like	signal transduction	-161.77
4	*nefh*	neurofilament heavy polypeptide	neurofilament cytoskeleton organization	-108.02
5	*muc5ac*	mucin-5ac- partial	cytoplasm	-107.85
6	*f11*	coagulation factor xi-like	regulation of blood coagulation	-89.65

7	*fut7*	alpha-( )-fucosyltransferase-like	integral component of membrane	-80.29
8	*mfap4*	microfibril-associated glycoprotein 4-like	protein binding	-73.63
9	*krt13*	type i cytoskeletal 13-like	protein binding	-67.46
10	*fel*	fish-egg lectin	cell	-53.68
11	*sema5b*	semaphorin-5b isoform x6	branching involved in blood vessel morphogenesis	-46.00
12	*urea*	urea transporter	urea transmembrane transport	-45.37
13	*c1ql4*	complement c1q-like protein 4 precursor	complement component C1q binding	-45.26
14	*cxcl14*	c-x-c motif chemokine 14 precursor	chemokine activity	-43.81
15	*cyp1*	cytochrome p450 1a	intracellular membrane-bounded organelle	-42.33
16	*hsd17b3*	testosterone 17-beta-dehydrogenase 3	intracellular membrane-bounded organelle	-35.82
17	*rasd2*	gtp-binding protein rhes-like	negative regulation of protein ubiquitination	-34.72
18	*igfbp-5*	insulin-like growth factor-binding protein 5-like	insulin-like growth factor binding	-29.01
19	*sfrp5*	secreted frizzled-related protein 5	negative regulation of canonical Wnt signaling pathway	-30.35
20	*vwc2*	von willebrand factor c domain-containing protein 2-like	AMPA glutamate receptor complex	-26.80

Supplementary Table 4 – List of top 20 Upregulated and Downregulated genes in head kidney of *D. labrax* infested with *A. ocellatum* representing gene symbol, protein product, gene ontology class and fold change.

UPREGULATED				
Ranking	**Gene symbol**	**Protein product**	**GO Class (Direct)**	**Fold change**
1	*mx*	interferon inducible mx protein	activation of innate immune response	4,867.73
2	*tuba1a*	tubulin alpha-1a chain	structural constituent of cytoskeleton	872.52
3	*rtp3*	receptor-transporting protein 3	protein binding	687.97
4	*ifn-alpha-1*	type alpha 1	B cell differentiation	270.30
5	*trim39*	e3 ubiquitin-protein ligase trim39-like	protein binding	129.68
6	*aste1*	protein asteroid homolog 1-like isoform x1	nuclease activity	98.21
7	*rgs5*	regulator of g-protein signaling 5-like	G protein-coupled receptor signaling pathway	70.16
8		inosine-uridine preferring nucleoside hydrolase-like	purine nucleoside catabolic process	56.72
9	*gad1*	glutamate decarboxylase-like protein 1	protein binding	55.83
10	*mx*	mx protein	innate immune response	48.64
11	*gig2*	gig2-like protein	cytoplasm	47.63
12	*rnp3*	nucleolar complex protein 3 partial	nucleolar ribonuclease P complex	43.45
13	*herc4*	probable e3 ubiquitin-protein ligase herc4-like	ubiquitin-protein transferase activity	43.34
14	*ddit4*	dna damage-inducible transcript 4	response to hypoxia	39.55
15	*cmpk2*	ump-cmp kinase mitochondrial	ATP binding	36.97
16	*ntf-2*	nuclear transport factor 2-like	positive regulation of antimicrobial peptide biosynthetic process	34.99
17	*irf3*	interferon regulatory factor 3	interferon-alpha production	34.75
18	*sntx*	stonustoxin subunit alpha	toxin activity	30.80
19	*angptl4*	angiopoietin-related protein 4-like	protein binding	28.68
20	*gimap7*	gtpase imap family member 7-like	GTPase activity	28.66
DOWNREGULATED				
Ranking	**Gene symbol**	**Protein product**	**GO Class (Direct)**	**Fold change**
1	*p13913*	arylamine n- pineal gland isozyme nat-10-like	arylamine N-acetyltransferase activity	-6,427.56
2	*dyrk1a*	dual specificity tyrosine-phosphorylation-regulated kinase 1a-like	peptidyl-tyrosine autophosphorylation	-787.65

3	*cpdb*	carboxypeptidase b	proteolysis involved in cellular protein catabolic process	-272.84
4	*prss1*	trypsin-1 precursor	proteolysis	-221.94
5	*ctrb1*	chymotrypsinogen 2	protein binding	-185.23
6	*try*	trypsinogen 2	proteolysis	-174.22
7	*cela2a*	chymotrypsin-like elastase family member 2a-like	proteolysis	-157.37
8	*hcea*	high choriolytic enzyme 1-like	metalloendopeptidase activity	-127.56
9	*mybpc1*	myosin-binding protein slow-type	myosin binding	-124.58
10	*actc1*	alpha cardiac-like isoform 1	atpase activity	-108.93
11	*ctn*	Cardiac troponin	troponin complex	-106.66
12	*cela1*	elastase-1-like	proteolysis	-76.32
13	*elsrp*	elastase-like serine protease	serine-type Endopeptidases inhibitor activity	-62.72
14	*serpinb1*	pancreatic elastase	type B pancreatic cell proliferation	-48.85
15	*tpm2*	tropomyosin beta chain-like isoform 1	protein binding	-44.62
16	*tcap*	telethonin	detection of muscle stretch	-43.25
17	*astl*	astacin like metallo-protease	cytoplasm	-40.78
18	*tnnc1*	troponin slow skeletal and cardiac muscles	troponin complex	-39.68
19	*pvalb7*	parvalbumin-7-like isoform x1	calcium ion binding	-35.21
20	*e7*	type i keratin e7	cytosol	-36.17